

GFZ

Helmholtz-Zentrum
POTSDAM

HELMHOLTZ-ZENTRUM POTSDAM

**DEUTSCHES
GEOFORSCHUNGSZENTRUM**

G. Grünthal, R. Arvidsson, Ch. Bosse

Earthquake Model for the European-Mediterranean Region for the Purpose of GEM1

Scientific Technical Report STR10/04

Imprint

HELMHOLTZ CENTRE POTSDAM
**GFZ GERMAN RESEARCH CENTRE
FOR GEOSCIENCES**

Telegrafenberg
D-14473 Potsdam

Published online in Potsdam, Germany
September 2010

ISSN 1610-0956

This work is published in the GFZ series
Scientific Technical Report (STR)
and is open accessible available at:
www.gfz-potsdam.de - News - GFZ Publications

G. Grünthal, R. Arvidsson, Ch. Bosse

Earthquake Model for the European-Mediterranean Region for the Purpose of GEM1

GFZ German Research Centre for Geosciences, Potsdam
Section 2.6 „Seismic Hazard and Stress Field“

September 2010

Scientific Technical Report STR10/04

Contents

1. Inducement and definition of the task	4
2. The seismicity data file	4
3. The SESAME seismic source zone model and its modification	6
4. The seismicity parameters of the source zones	14
4.1 <i>Seismicity data pre-processing</i>	14
4.2 <i>The frequency-magnitude parameters</i>	16
4.3 <i>The maximum expected magnitude m_{max}</i>	21
4.4 <i>The focal depth h</i>	22
5. The sanity check of the derived parameters in terms of a preliminary seismic hazard map	29
6. Conclusions	32
References	32

The PSHA input model provided with this report has been delivered to GEM1 in January 2010. The sanity check in form of a preliminary seismic hazard map has been updated in September 2010.

1. Inducement and definition of the task

The Global Earthquake Modelling project (GEM; www.globalquakemodel.org) requires in its starting phase GEM1 the use of existing and available earthquake models. The first earthquake model developed for the Euro-Mediterranean region is that of the Global Seismic Hazard Assessment Program GSHAP (*Giardini et al. 1999*). For the area north of 44°N represented by the GSHAP Region 3 (*Grünthal et al. 1999a*), a homogeneous earthquake model could be derived, while for the Mediterranean region, the GSHAP Region 4, a patchwork of regional approaches had to be assembled at the final stage of the project as a joint map (*Grünthal et al. 1999b*). A more homogeneous source zone model for the Mediterranean region was then developed within the IGCP ESC-project SESAME (*Jiménez et al. 2001*), where the different sub-regional models required minor adjustment in areas, where the different models join. At a later stage of the project SESAME, the data for the European part north of the Mediterranean developed for GSHAP (*Grünthal et al. 1999a*) had been added (*Jiménez et al. 2003*). Unfortunately, the seismicity parameters of the seismic source zones south of the GSHAP Region 3, i.e. the areas south of 44°N, are not accessible. Therefore, for the purpose of GEM1 the task was defined to provide the parameters of the seismic source zones. To these parameters belong:

- the geometry of the source zones,
- the frequency-magnitude parameters ν_0 and b ,
- the maximum expected magnitude m_{max} ,
- the focal depth h .

Since the Euro-Med part of GEM1 is represented by the EU-project SHARE, the study area is oriented according to the one defined for SHARE (Figure 1). The southeastern part of our model was extended to cover a larger part of Turkey (up to about 38°E) than the original SHARE study area of Figure 1. Reasons for this are, that the large source zones of central Turkey and the North and East Anatolian faults are considered as a homogeneous unit and should not be divided for hazard purposes.

In addition to the GEM1 requirements a first sanity check with respect to the earthquake model, particularly the frequency-magnitude parameter, has been performed in form of an elementary probabilistic seismic hazard assessment (PSHA). This preliminary seismic hazard calculation does not represent any final PSHA.

2. The seismicity data file

The seismicity data file used for this study is represented by the earthquake catalogue CENEC for Europe north of 44°N (*Grünthal et al. 2009a*). This paper describes in detail how this homogeneous data file in terms of moment magnitudes M_w (with $M_w \geq 3.5$) has been derived. The degree of harmonization achieved in CENEC is quantitatively analysed in *Grünthal et al. (2009b)*. The extension of CENEC to the south in connection with an update of

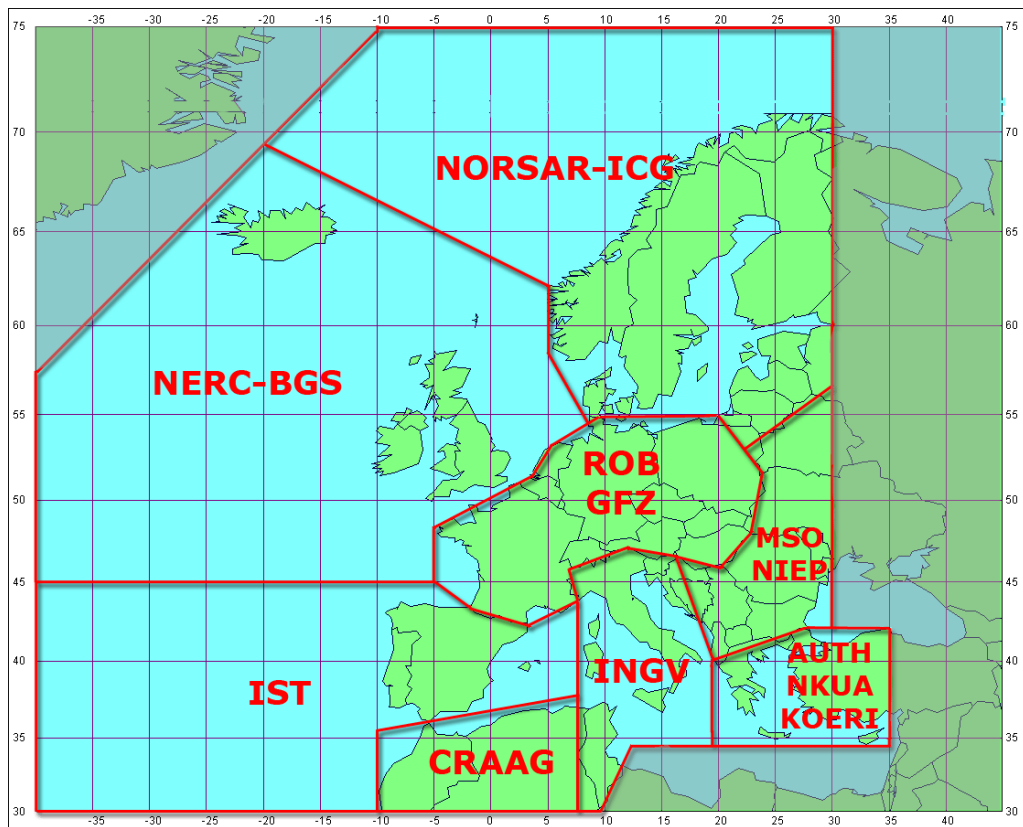


Figure 1. SHARE study area.

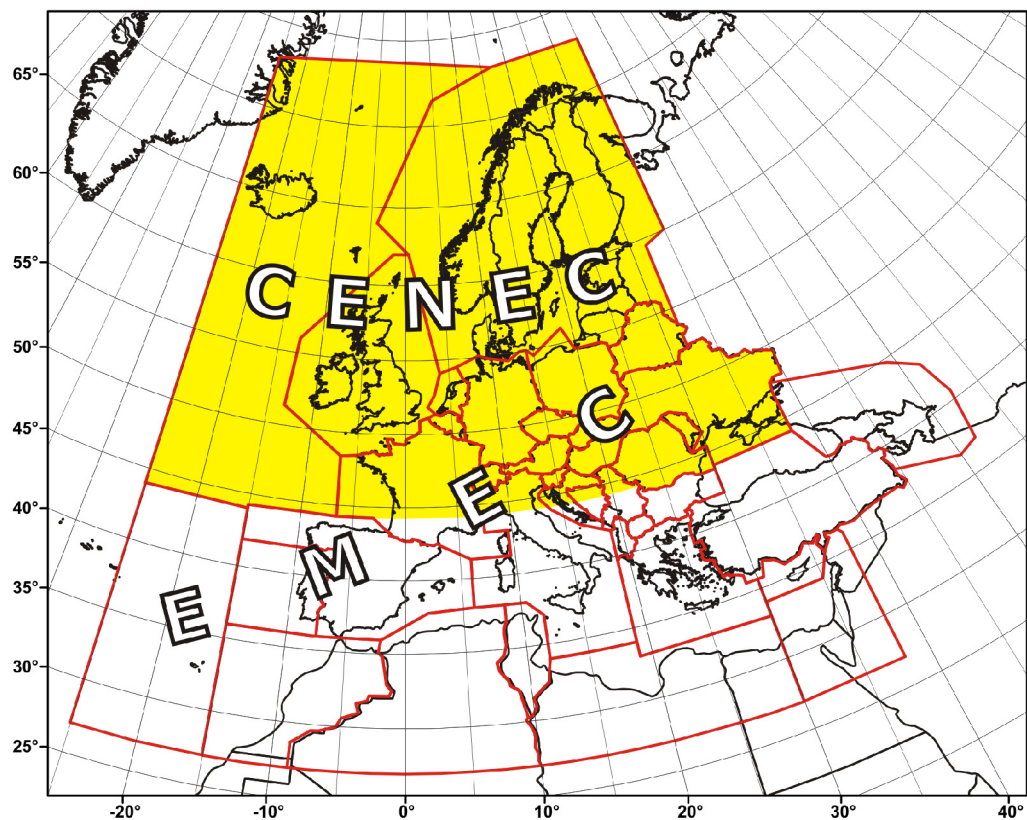


Figure 2. The polygons in each of which one or more of the catalogues and data bases are valid. The EMEC catalogue encompasses all polygons; CENEC covers the yellow-marked area.

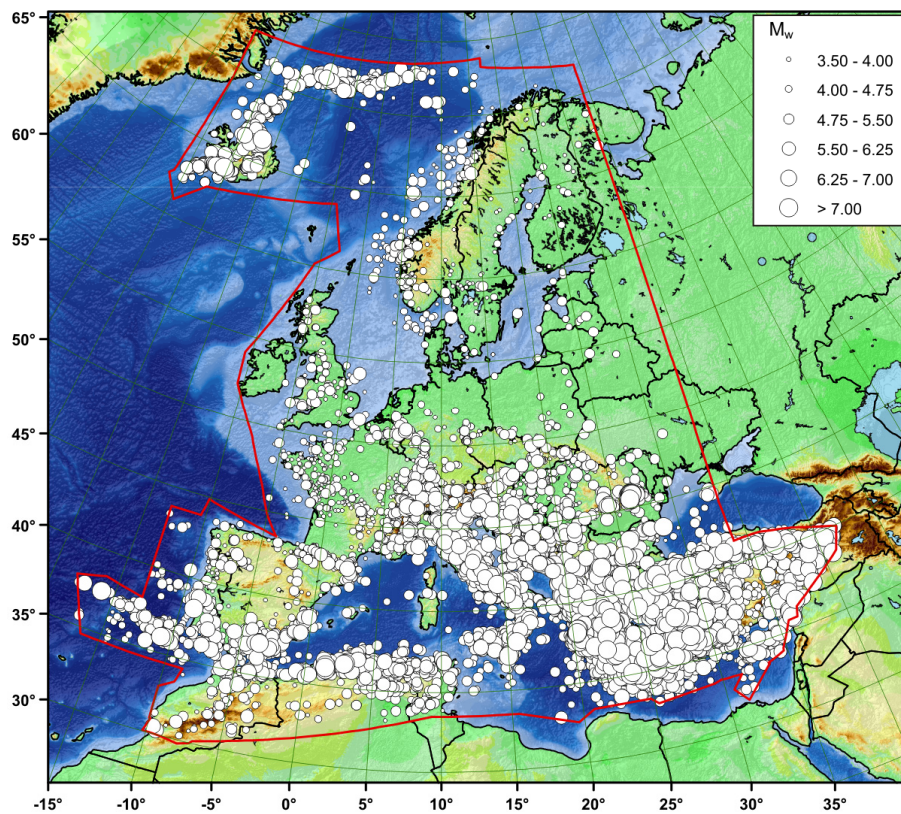


Figure 3. Epicentres of the seismicity data file CENEC and EMEC respectively used for this study in terms of M_w . The envelope within which the data are displayed follows from the outer border of the small scale seismic source zone model (cf. Fig. 5) and from the large scale zone model (cf. Fig. 7).

CENEC is represented by the Euro-Med earthquake catalogue EMEC, which is briefly discussed in Grünthal & Wahlström (2009). CENEC stands for Central, Northern and northwestern European earthquake Catalogue and EMEC for Euro-Mediterranean Earthquake Catalogue.

Figure 2 shows the areal polygons used for CENEC and EMEC. EMEC follows the same principles as used in CENEC. The lower threshold magnitude in the southern part of EMEC; i.e. south of the CENEC area, varies between $M_w = 3.5$ to $M_w = 4.5$. We make use of the stage of the project as per in November 2009 for preparing the harmonized seismicity data file. Figure 3 shows the appropriate map of epicentres in terms of harmonized M_w for the Euro-Med region sensu lato according to the interim file as described. A corresponding paper which characterizes the catalogue works in detail is under way. It will refer to the publicly available seismicity data file.

3. The SESAME seismic source zone model and its modification

According to the task for this study the basic seismic source zone (SSZ) model was that of SESAME (Jiménez *et al.* 2003), which is shown in Figure 4. For the study area of SHARE (Figure 1) the eastern and southeastern parts of the original SESAME SSZ model do not need to be considered here. This affects the SSZs for the area of Crimea, the western

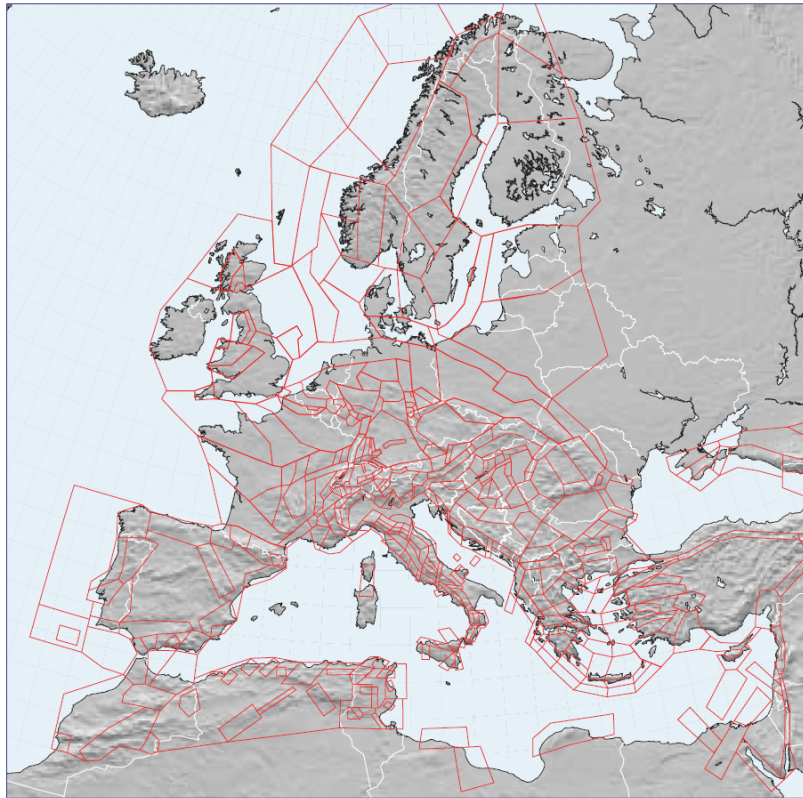


Figure 4. The SESAME seismic source zone (SSZ) model with 463 source zones (*Jiménez et al. 2003*).

Caucasus, the Near East, Libya and Egypt. On the other hand, the model had to be extended in the most western parts of the Eurasian plate, namely with respect to Iceland, and parts of the North Atlantic ridge SW and NE of Iceland. The resulting SSZ model of small scale zones for this study is shown in Figure 5a. Details of the SSZ model with the names of each zone are depicted in Figures 5b-k. The SESAME zonation for intermediate and deep seismicity was not modified in the current model. These are the seven ones along the Hellenic arc (Figure 5k) and the one zone for Vrancea. The entire SSZ model consists of 435 single source zones. Basically the SESAME SSZ model reflect national approaches. With respect to more details reference is given to *Jiménez et al. (2003)* or to the national studies respectively. It is not the subject of this study to retrieve and describe the justifications for distinguishing between different source zones.

Several large continuous areas in Figure 4, containing the western and eastern Mediterranean, the Adriatic Sea and the Po plain, were not covered with any SSZ in the initial SESAME model. In order to construct a model which does not include “holes”, new SSZs were introduced for those areas, which are by no means aseismic.

In the Hellenic Arc the seismicity for shallow SSZs is used down to a depth of 60 km and that for deeper SSZs below 60 km. For other parts of the Mediterranean events deeper than 50 km have a minor influence on the seismic hazard and were thus excluded from analysis.

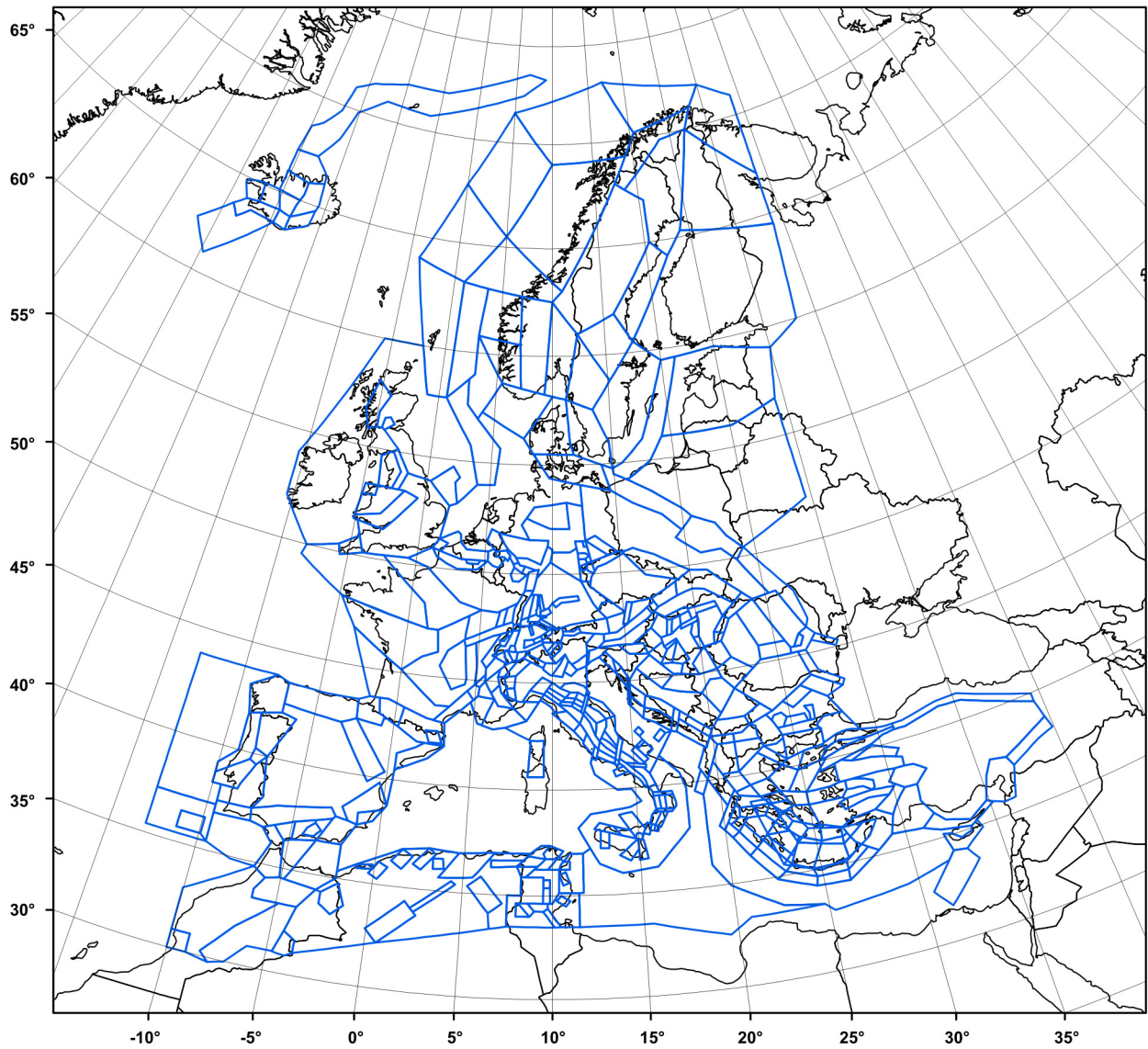


Figure 5a. The small scale seismic source zone (SSZ) model of this study. For details and the labelling of the source zones see the detailed maps (Figs. 5b-k).

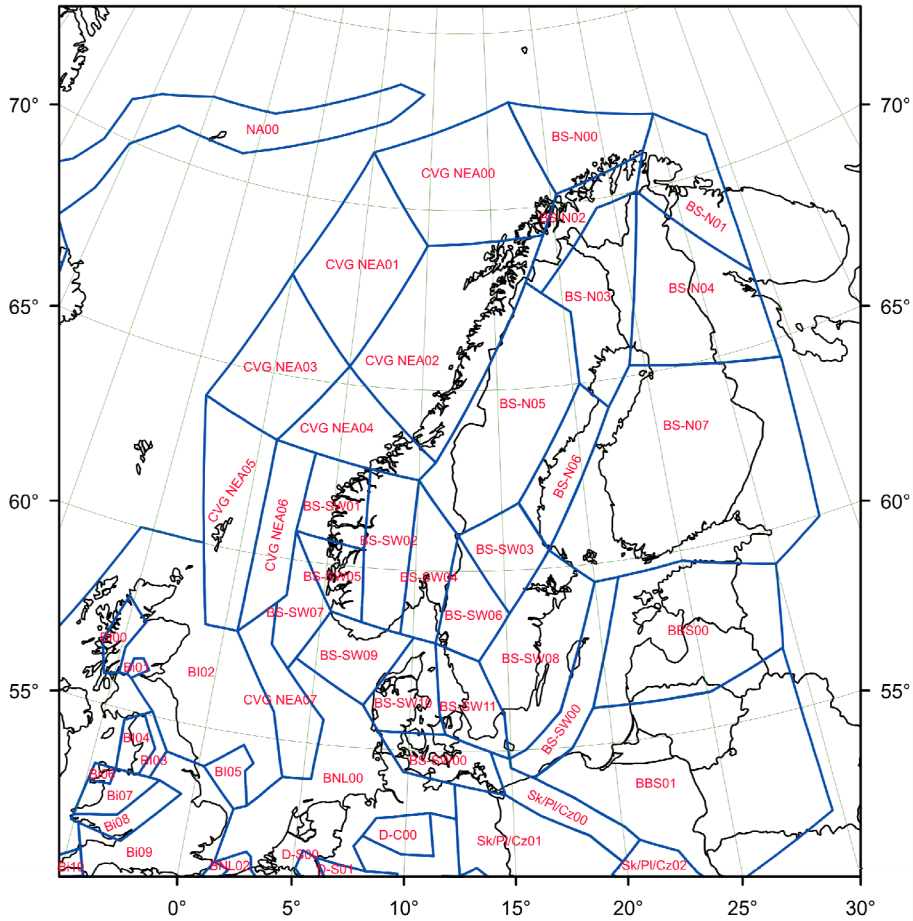


Figure 5b. Detailed SSZ model and labelling for Fennoscandia and N Europe.

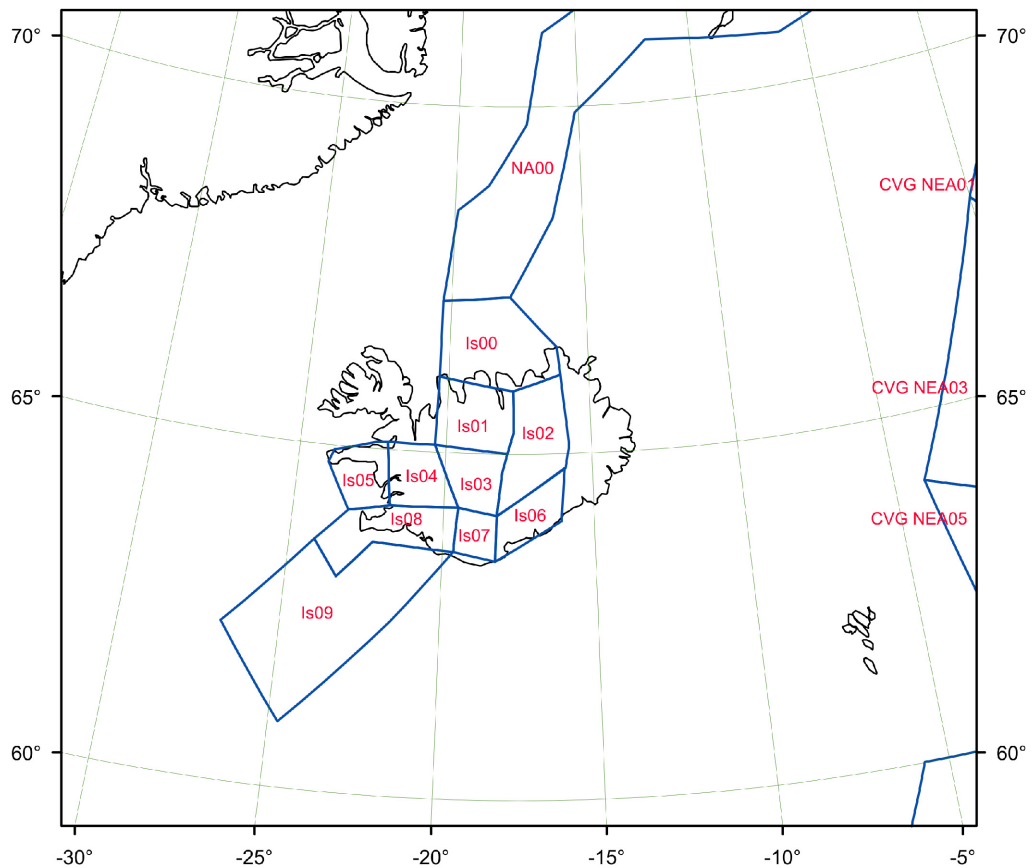


Figure 5c. Detailed SSZ model and labelling for Iceland and part of the North Atlantic Ridge.

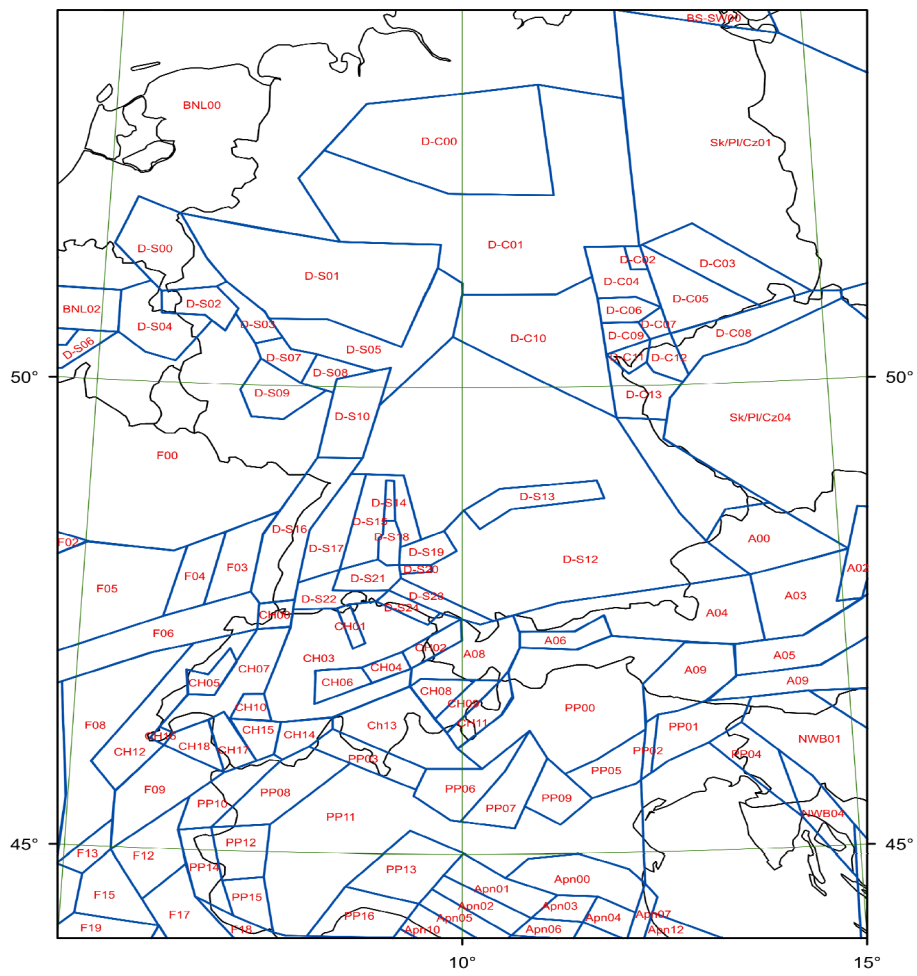


Figure 5d. Detailed SSZ model and labelling for W Central Europe.

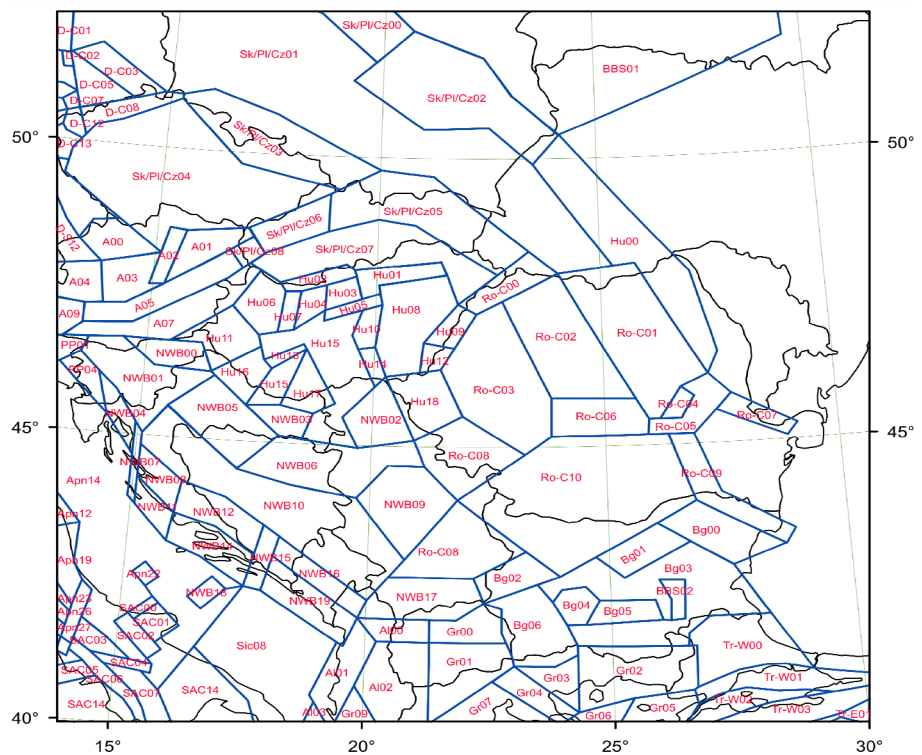


Figure 5e. Detailed SSZ model and labelling for SE Central Europe and N Balkan.

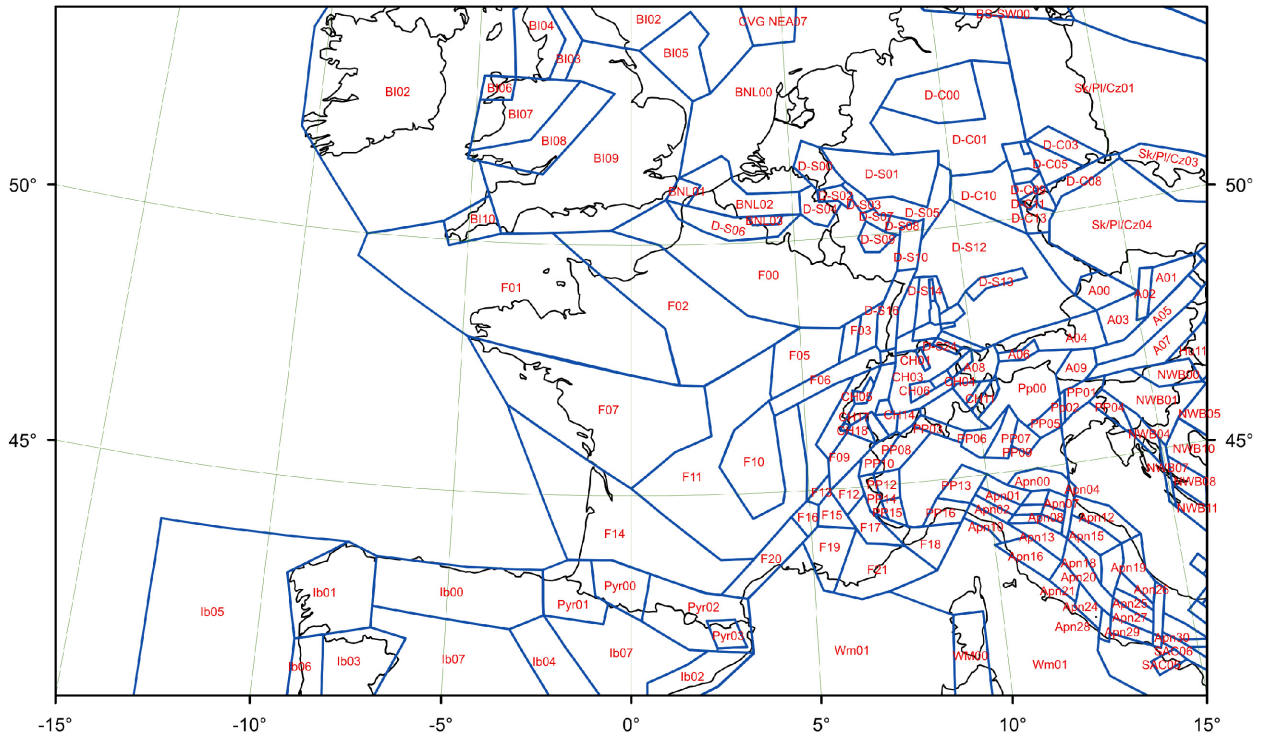


Figure 5f. Detailed SSZ model and labelling for W Europe.

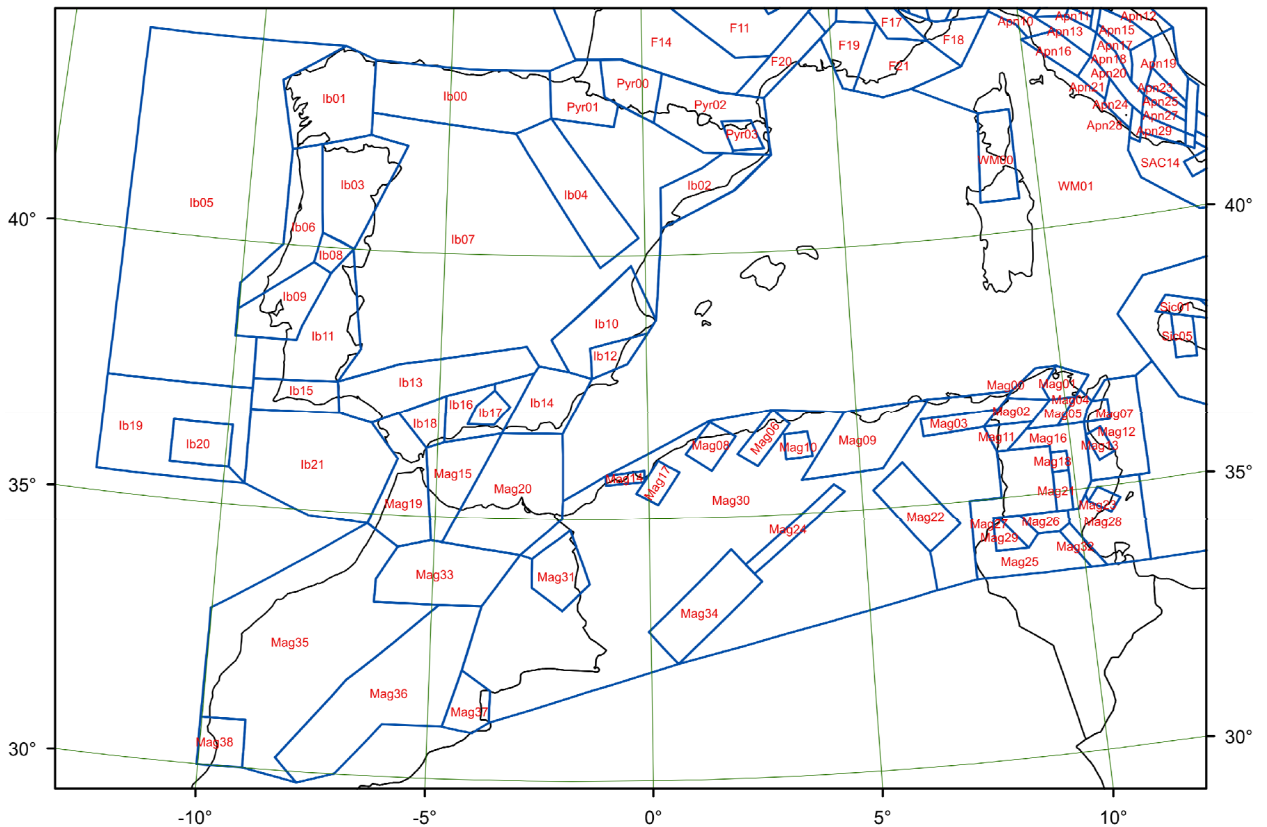


Figure 5g. Detailed SSZ model and labelling for SW Europe and Maghreb.

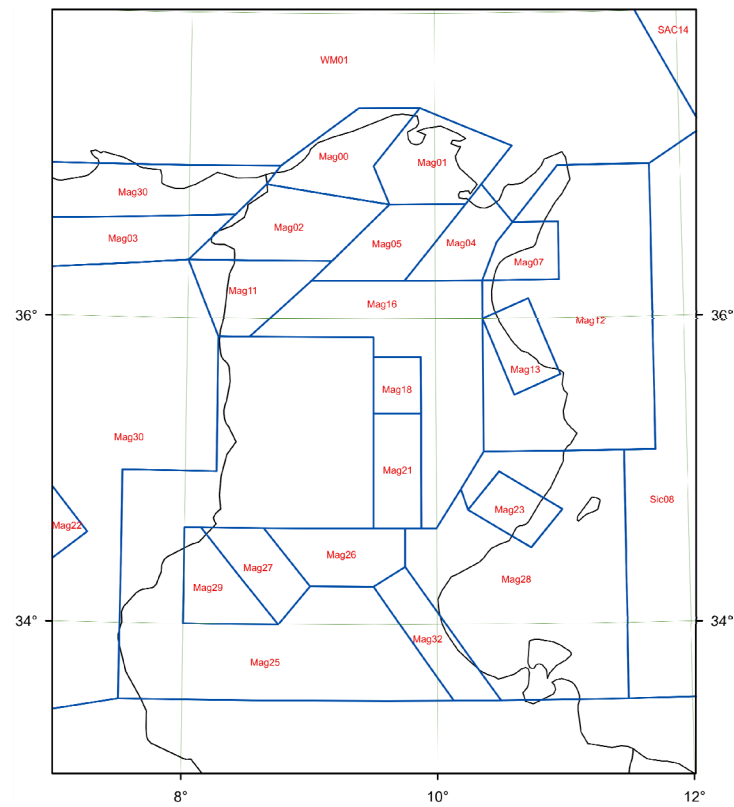


Figure 5h. Detailed SSZ model and labelling for Tunisia.

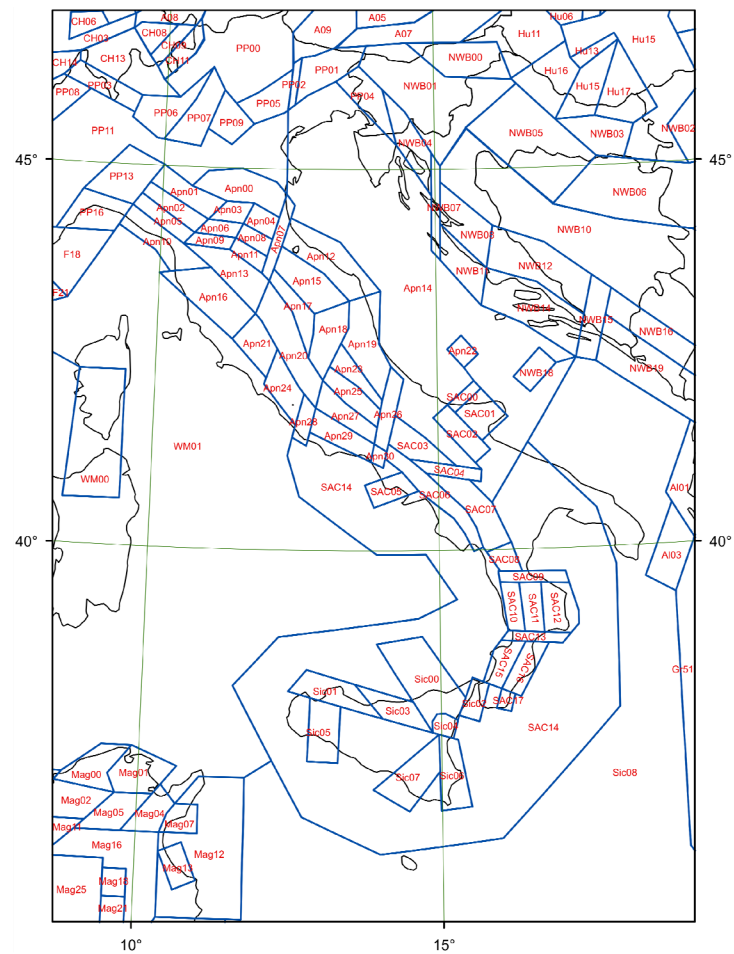


Figure 5i. Detailed SSZ model and labelling for Italy and NW Balkan.

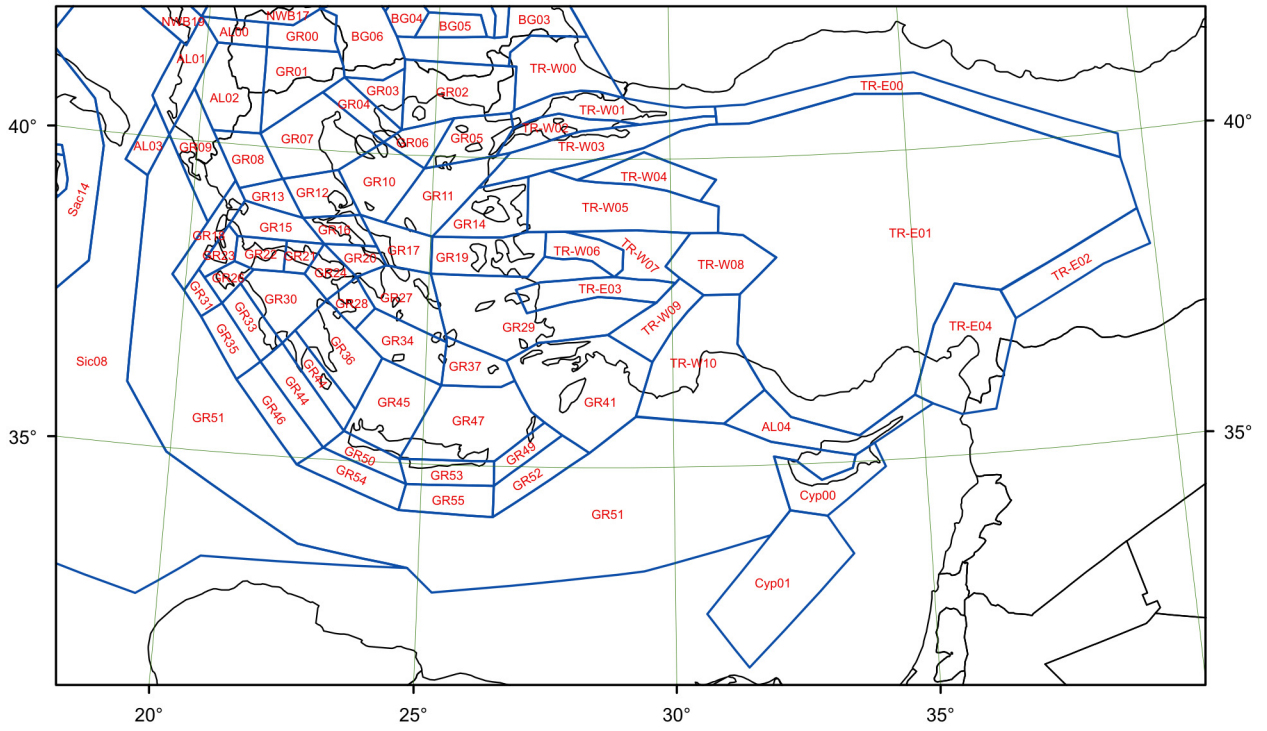


Figure 5j. Detailed SSZ model and labelling for S Balkan, E Mediterranean, W and central Turkey.

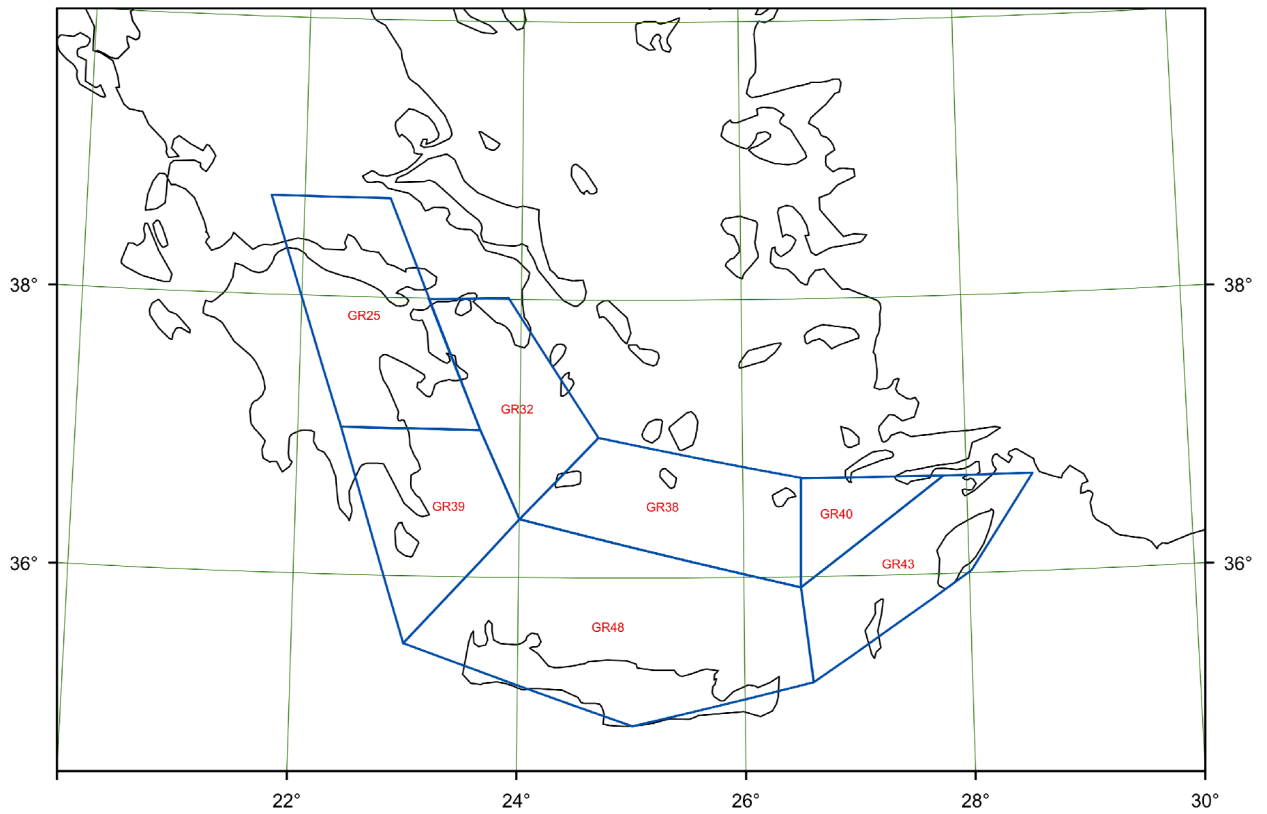


Figure 5k. Intermediate depth SSZ model for the Aegean arc.

4. The seismicity parameters of the source zones

4.1 Seismicity data pre-processing

The seismicity data pre-processing consists of two steps: Firstly, the declustering, i.e. the removal of foreshocks and aftershocks, and secondly, the analysis of data completeness with time.

The declustering applied here follows the robust and rigorous method by Grünthal from 1985, which was extended to apply to larger magnitudes, as described by *Burkhard & Grünthal (2009)* and *Grünthal et al. (2009a)*. Although originally developed for central European conditions, the method proved to be equally applicable for a study for the Levant (*Grünthal et al. 2009b*) and it will be used here as well. The effect of declustering is illustrated in Figure 6. While the effect of declustering is indeed drastical up to $M_w = 5.0$, it is negligible for $M_w \geq 6.0$.

The analysis of magnitude-dependent data completeness with time follows the standard methodology we successfully applied for more than 20 years. Since this approach has frequently been described in previous publications (e.g. *Burkhard & Grünthal 2009* or *Suckale & Grünthal 2009*) we can be brief here. Basically, a magnitude bin is considered complete for the years in which a constant slope can be fitted to the cumulative number of earthquakes. The application of this approach to the entire Euro-Med study region requires first of all the differentiation into sub-regions with their characteristic seismicity features. This delineation into large scale zones for the purpose of (1) completeness analysis and (2) common- b areas (Section 4.2) is shown in Figure 7. Table 1 provides the full names of these sub-regions with their abbreviations used in Figure 1. The temporal completeness for each magnitude class in each of the sub-regions is given in Table 2.

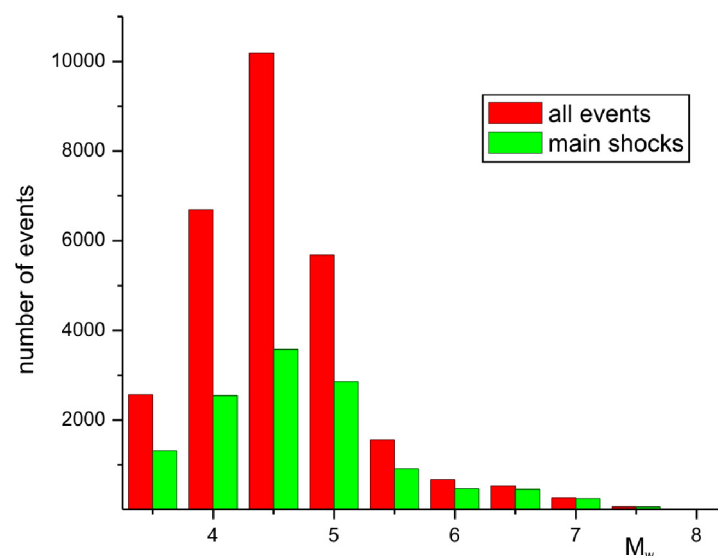


Figure 6. Effect of declustering of the used data set study. The number of events per magnitude class for the non-declustered data is shown by red columns and for the declustered data by green columns.

Table 1. Large scale zones as shown in Fig. 7 for completeness analysis and applied as common-*b* zones as well (Section 4.2).

short form	full name	short form	full name
A	Austria	Hu	Hungary
Al	Albania	Ib	Iberian Peninsula
Apn	Apennines	Is	Iceland
BBS	Baltic Republics and Baltic Shield	Mag	Maghreb
Bg	Bulgaria	NA	Northern Atlantic
BI	British Islands	NWB	North and Western Balkan
BNL	BeNeLux	PP	Po plain
BS-N	Baltic Shield North	Pyr	Pyrenees
BS-SW	Baltic Shield South-West	Ro-C	Romania crustal
CH	Switzerland	Ro-D	Romania deep
CVG NEA	Central and Viking graben and NE Atlantic	SAC	Southern Apennines and Calabria
Cyp	Cyprus	Sic	Sicily
D-C	Central Germany	Sk/Pl/Cz	Slovakia / Poland / Czech Republic
D-S	Southern and Western Germany	Tr-E	Turkey East
F	France	Tr-W	Turkey West
Gr	Greece	WM	Western Mediterranean Sea

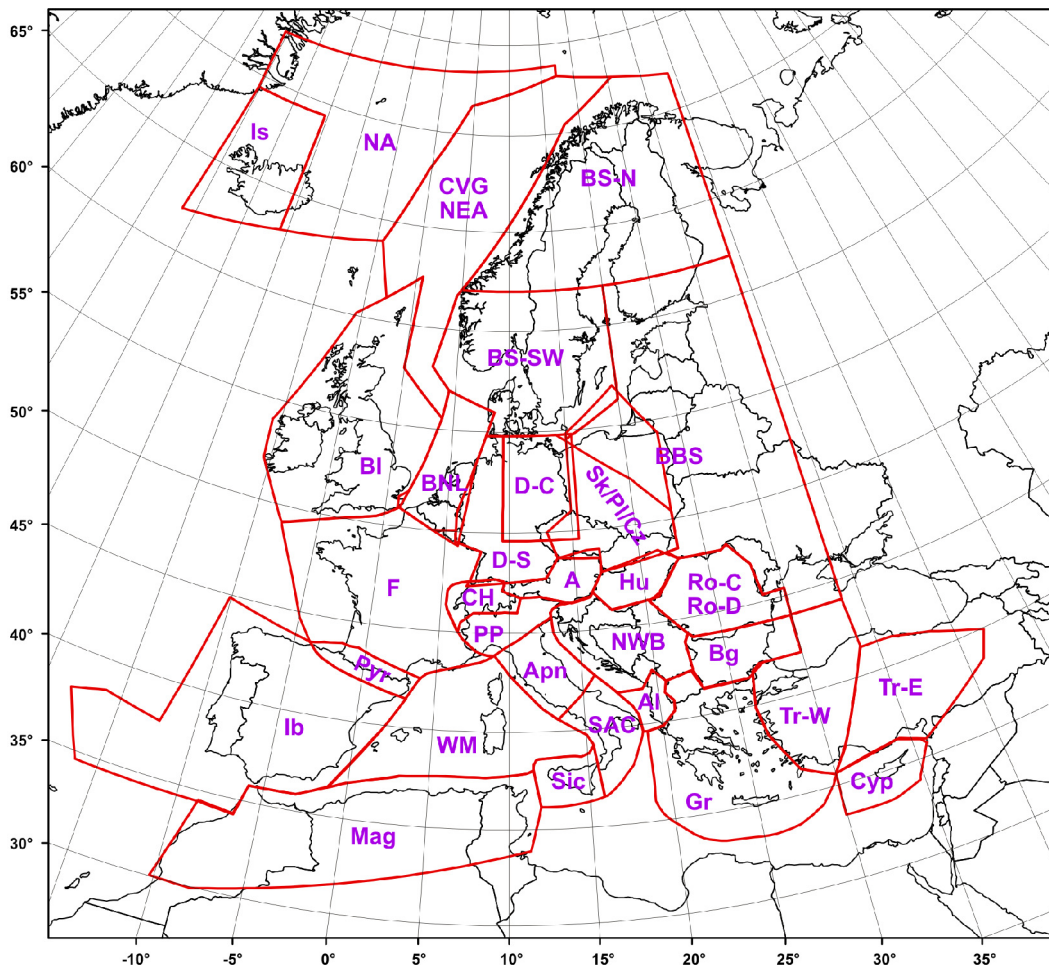


Figure 7. The large scale zone model developed for the determination of data completeness with time and for the use as common-*b* area in case of seismic source zones with scarce seismicity data.

Table 2. The temporal completeness for each magnitude class in each of the sub-regions given in Tab. 1 and Fig. 7.

	3.5	4.0	4.5	5.0	5.5	6.0	6.5	7.0	7.5	8.0
A	1895	1850	1800	1760	1550	1400	1400			
Al		1980	1970	1963	1920	1855	1830	1700		
Apn			1950	1875	1780	1400	1400	1000		
BBS	1955	1890	1890	1850	1800	1800				
Bg	1930	1900	1900	1900	1900	1800	1700	1700		
BI	1970	1875	1865	1840						
BNL	1925	1890	1860	1860	1300	1300				
BS-N	1963	1880	1880	1800	1800	1800				
BS-SW	1970	1880	1880	1800	1700					
CH	1880	1860	1825	1770	1650	1575	1250	1250		
CVG NEA	1981	1955	1950	1900	1860	1850				
Cyp		1983	1964	1920	1900	1900	1000	800	800	800
D-C	1850	1675	1500	1300	1300	1300				
D-S	1925	1875	1870	1820	1600	1500	1500	1250		
F	1930	1925	1925	1800	1650					
Gr			1963	1963	1910	1910	1700	1500	1500	1400
Hu	1860	1840	1800	1800	1700	1700				
Ib		1950	1950	1950	1950	1820	1750	1650	1350	1350
Is		1990	1955	1955	1920	1920	1870	1730		
Mag		1950	1950	1920	1920	1870	1700	1700	1700	
NA		1990	1975	1975	1920	1900	1900	1900		
PP			1900	1875	1780	1400	1400	1000		
Pyr	1970	1920	1860	1850	1850	1350	1350			
Ro-C	1970	1890	1890	1890	1750	1700	1500	1500	1500	
Ro-D	1990	1990	1990	1950	1925	1900	1775	1500	1100	
SAC			1900	1840	1820	1750	1550	1550		
Sic			1960	1910	1910	1750	350	350		
Sk/Pl/Cz	1920	1920	1850	1760	1750	1750				
Tr-E		1995	1963	1950	1900	1900	1800	1800	1800	1200
Tr-W		1975	1970	1960	1900	1900	1600	1600	1200	1200
WM			1975	1900	1900	1900				
NWB	1900	1900	1900	1840	1840	1840	1280	1280		

4.2 The frequency-magnitude parameters

A SSZ is described, additional to its geometry, by three seismic activity parameters:

- ν_0 : the average yearly rate of events above or equal to a minimum magnitude m_0 ,
- b, β : the negative slope of the logarithm of the yearly rate depending on the magnitude,
- m_{max} : the maximum expected magnitude.

The non-cumulative frequency-magnitude relation $N(m)$ is in its classical form defined as the Gutenberg-Richter relation (*Gutenberg & Richter 1954*)

$$\log N(m) = a - b m . \quad (1)$$

In exponential form the non-cumulative rate ν reads

$$\nu_{nc}(m) = \exp(\alpha - \beta m) = 10^{a-b m} . \quad (2)$$

This relation holds within the magnitude range $m < m_{max}$. $exp(\alpha)$ is the value of v_{nc} at $m = 0$. The cumulative yearly frequency $v(m)$ under consideration of m_0 and m_{max} is

$$v(m) = v_0 \frac{exp[\beta * (m_{max} - m)] - 1}{exp[\beta * (m_{max} - m_0)] - 1} \quad m_0 \leq m \leq m_{max} \quad (3)$$

with $\beta = b \cdot \ln(10)$.

The parameters v_0 and b (respective β) have been determined with the maximum-likelihood estimation after *Weichert* (1980). The calculation of these parameters was no straightforward undertaking in areas of low seismic activity. This difficulty arose due to the combination of the small areal extent of many SSZs with the given lower magnitude thresholds of the data file. In cases where the number of data within an SSZ is not sufficient for a meaningful calculation of the frequency-magnitude parameter (less than 50 events), the b -value of an appropriate large scale zone is adopted for the respective SSZ. The respective v_0 -value is then determined by the best fit to the data in that particular small scale SSZ. The large scale zones used for assigning b -values to SSZs with too small amount of data are either the large scale zones shown in Figure 7 or even a combination of them. It proved to be necessary to introduce two of such combinations: BBS+D-C+Sk/Pl/Cz and BI+BNL+CVG NEA. The cases where b stems from a common- b zone are marked by an asterisk at the respective values in Table 3. This table summarizes the values for all parameters derived for each SSZ: b , the cumulative annual rate at $M_w = 3.8$, the focal depth, and the upper bound magnitude. A detailed picture of the locations of the SSZs in Table 3 is given with the Figures 5b-k. Figures 8-14 show examples of cumulative frequency-magnitude graphs for SSZs: three for Greece, and one each for Turkey, Vrancea, NW Balkan, and Italy. Figures 15 and 16 represent the cumulative frequency-magnitude for two large scale zones for Italy.

There exist SSZs which remain “empty”. They have been divided into two groups: (1) SSZs without any event above the threshold magnitude of the catalogued data and (2) SSZs containing events from the used catalogue, but without events of the complete part of the catalogue.

The SSZs of the first group are: BNL00, BS-SW00, CVG NEA05, CVG NEA07, D-C00, D-C03, D-S11, D-S23, Mag28, Mag31, and Sk/Pl/Cz04. No parameters could be assigned to them. The second group of SSZs covers catalogued seismicity, but the SSZs are represented by seismic events which occurred before the respective magnitude-dependent catalogue-completeness times. For such zones a conservative approach in calibrating the associated v -value was applied. The respective cumulative frequency-magnitude relation with the b -value adopted from the common- b area has been calibrated with respect to the corresponding v -value at the lower bound of the appropriate magnitude class being the reciprocal of its completeness time. It has always been chosen for the respective magnitude completeness class which yields the smallest value of v_0 .

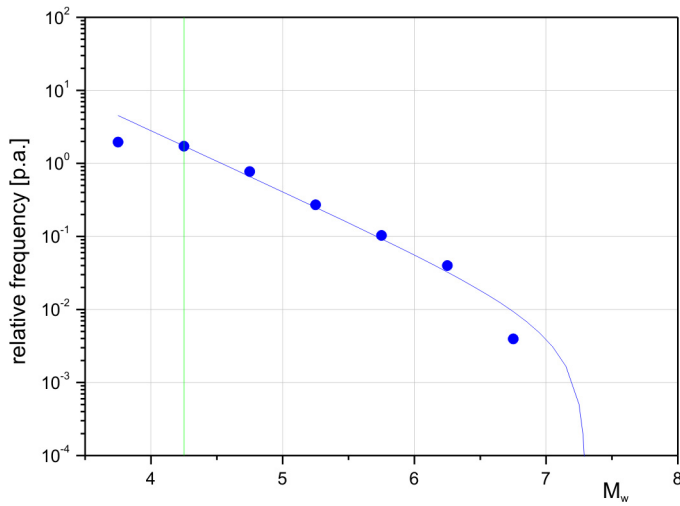


Figure 8. Frequency-magnitude relation for the SSZ Gr09 (Greece). The b -value with its standard deviation is 0.833 ± 0.055 . The frequency rate $\nu(M_w = 4.25)$ is 1.732. The green line marks the threshold in M_w for calculating ν and b .

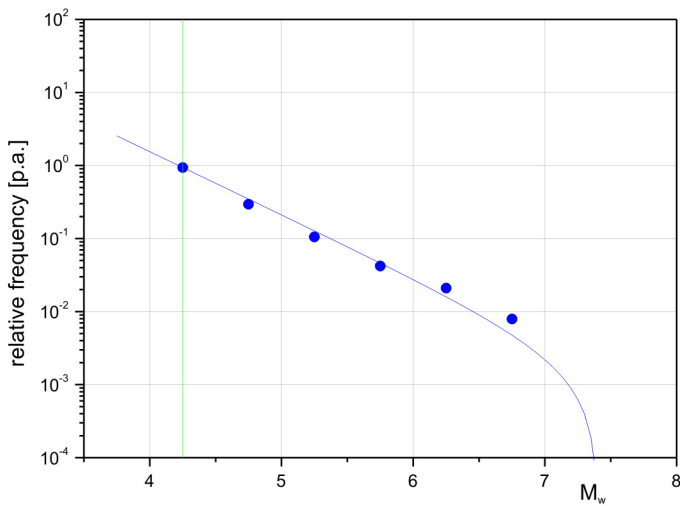


Figure 9. Frequency-magnitude relation for the SSZ Gr14 (Greece). $b = 0.863 \pm 0.078$, $\nu(M_w = 4.25) = 0.941$.

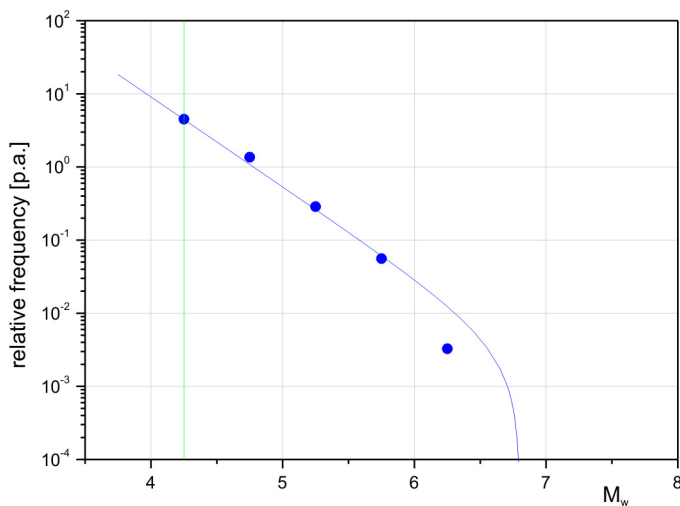


Figure 10. Frequency-magnitude relation for the SSZ Gr51 (Greece). $b = 1.228 \pm 0.063$, $\nu(M_w = 4.25) = 4.462$.

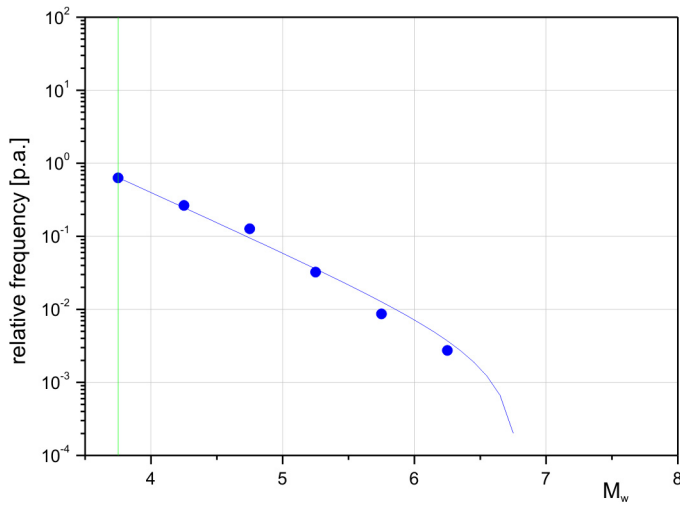


Figure 11. Frequency-magnitude relation for the SSZ NWB01 (NW Balkan).
 $b = 0.819 \pm 0.072$, $\nu(M_w = 3.75) = 0.638$.

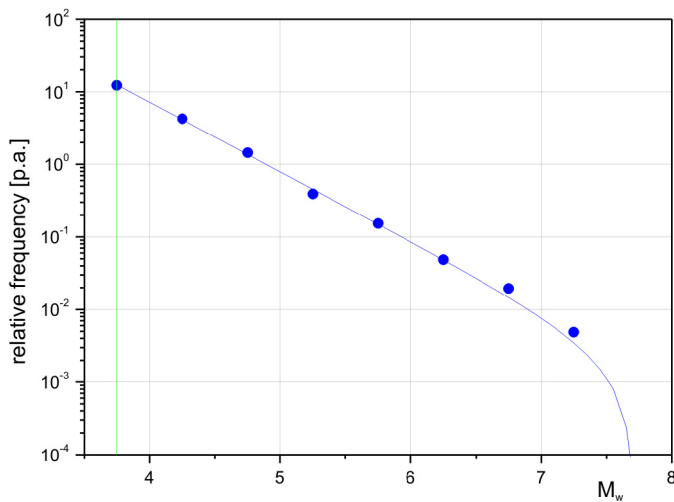


Figure 12. Frequency-magnitude relation for the SSZ Tr_E01 (central Turkey).
 $b = 0.958 \pm 0.038$, $\nu(M_w = 3.75) = 12.456$.

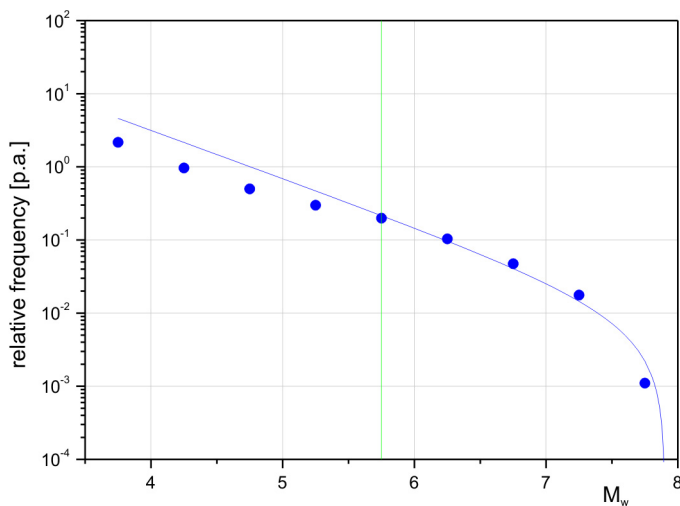


Figure 13. Frequency-magnitude relation for the intermediate depth SSZ Ro-D00 (Romania deep).
 $b = 0.657 \pm 0.092$, $\nu(M_w = 5.75) = 0.215$.

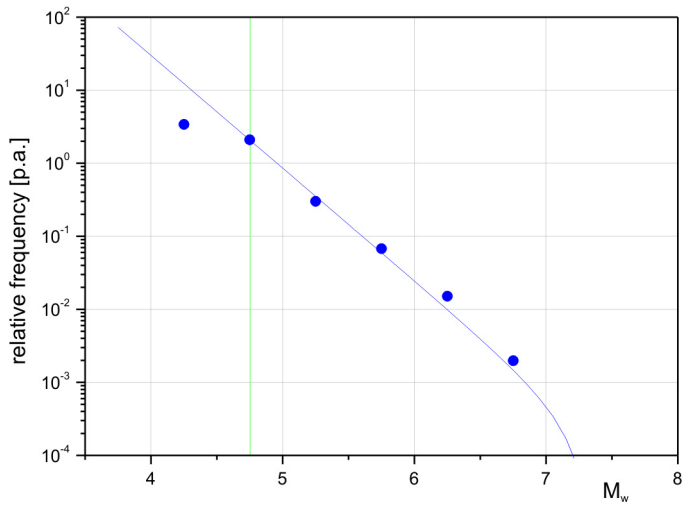


Figure 14. Frequency-magnitude relation for the SSZ SAC14.

$b = 1.449 \pm 0.173$, $\nu(M_w = 4.75) = 0.338$.

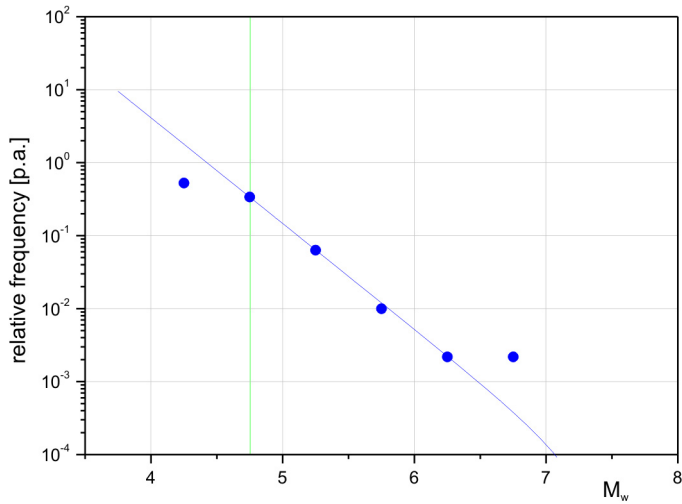


Figure 15. Frequency-magnitude relation for the large scale zone Aprn.

$b = 1.543 \pm 0.062$, $\nu(M_w = 4.75) = 2.084$.

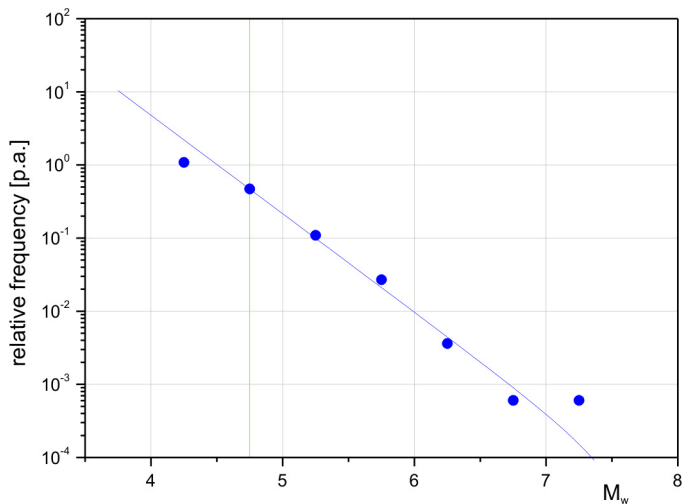


Figure 16. Frequency-magnitude relation for the large scale zone Sic.

$b = 1.346 \pm 0.100$, $\nu(M_w = 4.75) = 0.468$.

The b -values are in the range from 0.66 to 1.68 with a mean $b = 1.05$ for the shallow zones. For intermediate depth SZ the range in b is from 0.66 to 0.8 with a mean of 0.78. The highest b -values of 1.54 and 1.68 are observed within the two large zone areas of Italy, Apn (Apennines) and PP (Po plain). These high b -values of especially northern Italy are also found by *Gulia & Meletti* (2008). Three different examples of b -values are shown in Figures 14-16, two from large scale zones (Apn, Sic – Sicily) and one from SSZs (SAC14 belonging to the large scale zone Southern Apennines and Calabria), having b -values larger than 1.3. All show a fairly good fit to the frequency-magnitude relation.

4.3 The maximum expected magnitude m_{max}

The aim in the present study for determining m_{max} has been to achieve a homogenous estimate of this parameter throughout the area if possible. From previous studies there are known several approaches for determining m_{max} . In the north, in the stable continental regions, the m_{max} determination (e.g., see *NORSAR & NGI* 1998, *Wahlström & Grünthal* 2001, *Grünthal & Wahlström* 2006, *Burkhard & Grünthal* 2009) has often been based on an EPRI type methodology (*Coppersmith* 1994, *Cornell* 1994) which is applicable to stable continental crust, subdivided into non-extended and extended. The EPRI method replaces temporal limitations of the earthquake record in seismically less active stable continental regions by space in form of global prior distribution functions of maximum observed magnitudes specified for the mentioned crustal types.

The determination of m_{max} along active plate boundaries as in the Mediterranean, has, on the other hand, often been based on the assumption that given a sufficient long catalogue of observed events, the maximum magnitude earthquake should have occurred. Thus, often m_{max} has been set to the observed maximum magnitude (e.g., see *Rebez & Slejko* 2004, *Papouannou & Papazachos* 2000) or maximum observed magnitude plus a small increment (e.g., see *Slejko et al.* 1998, *Musson* 1999) as well as statistical estimates from, e.g., the *Kijko & Graham* (1998) method (e.g., *Rebez & Slejko* 2004).

For the north the minimum m_{max} given in the studies of *Musson & Sargeant* (2007), *Wahlström & Grünthal* (2001), *Norsar & NGI* (1998), is $M_w = 5.5$, 5.4 and 6.0, respectively. Thus, a realistic minimum of the m_{max} for this region is about 5.5. It was judged that such an event, though not of high probability could occur anywhere within this region.

In the last official Italian earthquake model ZS 9 (*Meletti et al.* 2008) the minimum value for m_{max} was considered to be $M = 5$. This is, in contrast to the northern values, low. It was deemed improbable that a smaller lowest m_{max} threshold for the more tectonically active regions of the Mediterranean can occur. Therefore, a magnitude 5.5 as a pan-European value for the minimum value of m_{max} was assumed.

Taking the above estimates into consideration there was adopted the approach of deriving m_{max} by adding an increment of 0.3 to the magnitude of the largest observed earthquake in a SSZ. If this maximum observed magnitude then was lower than 5.2, m_{max} was

set to 5.5. In SSZs along the Hellenic Arc, Gr33, Gr44, Gr49, Gr50, Gr53, it was assumed that the observed maximum magnitude of 8.3 along the arc is valid. No increment was added for these zones. In the large source zones of the background seismicity type with very scarce seismic activity (PP11, Apn14, Sic08 and WM01, i.e. in the Po plain, the Adriatic Sea and Western Mediterranean), the observed maximum magnitude was set as m_{max} . All m_{max} values are shown in Table 3.

4.4 The focal depth h

Initially, the average focal depth was determined for all SSZs. Here the average of the five largest events in an SSZ was calculated. However, often erroneous or poorly constrained depths made the results unreliable, since these events were not easily distinguished from earthquakes with well constrained depths. Therefore, for all SSZs representing shallow seismicity, a default value of 12 km was adopted as an average focal depth (Table 3).

For the intermediate and deeper SSZs in the Hellenic Arc, the depth of the seismic source zones was set to 80 km or 130 km, corresponding to the average depth of the model of *Papaioanniou & Papazachos* (2000). The Romanian intermediate depth source zone Ro-D00 on the other hand, has more reliable depth estimations from seismicity and therefore the average depth of events with $M_w \geq 7.5$ was used (Table 3).

Table 3. Frequency-magnitude parameter values in the seismic source zones (SSZ): The Gutenberg-Richter b -value and the corresponding ν at $M_w = 3.8$ - * indicates that the corresponding data have been derived for a common- b zone - the adopted focal depth h , and maximum expected magnitude m_{max} .

Title	b	$\nu(3.8)$ [p.a.]	h [km]	m_{max}
A00	0.9071*	0.004815*	12	5.5
A01	0.9071*	0.1214*	12	6.5
A02	0.9071*	0.02241*	12	5.5
A03	0.9071*	0.02408*	12	5.5
A04	0.9071*	0.02408*	12	5.5
A05	0.8202	0.2311	12	6.0
A06	0.9071*	0.0849*	12	5.9
A07	0.9071*	0.009631*	12	5.5
A08	0.9071*	0.06745*	12	5.6
A09	0.9071*	0.009347*	12	6.9
Al00	0.8705*	1.132*	12	7.3
Al01	0.8705*	2.939*	12	7.0
Al02	0.9162	4.07	12	7.1
Al03	0.8705*	0.4564*	12	7.2
Al04	0.8705*	0.5664*	12	6.6
Apn00	1.543*	2.067*	12	6.1
Apn01	1.543*	3.194*	12	6.1
Apn02	1.543*	0.954*	12	5.8
Apn03	1.543*	1.326*	12	5.9
Apn04	1.543*	3.169*	12	6.2
Apn05	1.543*	2.939*	12	6.8
Apn06	1.543*	1.473*	12	5.6
Apn07	1.543*	1.11*	12	6.3

Table 3. continued				
Title	<i>b</i>	<i>v</i>(3.8) [p.a.]	<i>h</i> [km]	<i>m</i>_{max}
Apn08	1.543*	3.186*	12	6.2
Apn09	1.543*	0.3484*	12	5.5
Apn10	1.543*	0.1394*	12	5.5
Apn11	1.543*	1.107*	12	6.6
Apn12	1.543*	3.86*	12	6.1
Apn13	1.543*	1.879*	12	6.1
Apn14	1.543*	5.353*	12	6.5
Apn15	1.543*	1.134*	12	6.6
Apn16	1.543*	2.02*	12	6.9
Apn17	1.543*	3.135*	12	6.7
Apn18	1.543*	8.264*	12	7.0
Apn19	1.543*	2.214*	12	6.6
Apn20	1.543*	1.837*	12	6.9
Apn21	1.543*	1.687*	12	6.2
Apn22	1.543*	0.43*	12	5.5
Apn23	1.543*	1.836*	12	7.0
Apn24	1.543*	1.037*	12	5.7
Apn25	1.543*	1.651*	12	7.3
Apn26	1.543*	1.836*	12	7.1
Apn27	1.543*	3.122*	12	6.9
Apn28	1.543*	1.717*	12	5.8
Apn29	1.543*	0.3789*	12	5.9
Apn30	1.543*	0.5684*	12	5.9
BBS00	0.8321*	0.03595*	12	5.5
BBS01	0.8321*	0.02876*	12	5.5
BBS02	0.8321*	0.05*	12	6.0
Bg00	0.7021*	0.08894*	12	6.9
Bg01	0.7021*	0.1881*	12	7.4
Bg02	0.7021*	0.1561*	12	6.8
Bg03	0.7021*	0.1738*	12	6.1
Bg04	0.7021*	0.07575*	12	5.5
Bg05	0.7021*	0.1773*	12	7.4
Bg06	0.8502	0.4304	12	7.5
BI00	1.098*	0.09288*	12	5.5
BI01	1.098*	0.007813*	12	5.5
BI02	1.098*	0.006634*	12	5.5
BI03	1.098*	0.06662*	12	5.5
BI04	1.098*	0.01327*	12	5.5
BI05	1.098*	0.01991*	12	6.2
BI06	1.098*	0.08882*	12	5.5
BI07	1.098*	0.07857*	12	5.5
BI08	1.098*	0.2443*	12	5.5
BI09	1.098*	0.04441*	12	5.5
BI10	1.098*	0.01327*	12	5.5
BNL01	1.098*	0.01266*	12	5.8
BNL02	1.098*	0.08228*	12	6.2
BNL03	1.098*	0.159*	12	5.5
BS-N00	1.155*	0.006612*	12	5.5
BS-N01	1.155*	0.006612*	12	5.5
BS-N02	1.155*	0.0231*	12	5.5
BS-N03	1.155*	0.006612*	12	5.5
BS-N04	1.155*	0.1155*	12	5.5
BS-N05	1.155*	0.01322*	12	5.5
BS-N06	1.155*	0.03306*	12	5.5
BS-N07	1.155*	0.02645*	12	5.5
BS-SW01	1.086	0.3465	12	5.5
BS-SW02	1.155*	0.02618*	12	5.5
BS-SW03	1.155*	0.006544*	12	5.5
BS-SW04	1.155*	0.03929*	12	5.7
BS-SW05	1.155*	0.144*	12	5.5
BS-SW06	1.155*	0.01963*	12	5.5
BS-SW07	1.155*	0.006544*	12	5.5
BS-SW08	1.155*	0.007091*	12	5.5

Table 3. continued				
Title	<i>b</i>	$\nu(3.8)$ [p.a.]	<i>h</i> [km]	m_{max}
BS-SW09	1.155*	0.1178*	12	5.5
BS-SW10	1.155*	0.01304*	12	5.9
BS-SW11	1.155*	0.01309*	12	5.5
CH00	0.8364*	0.04068*	12	7.2
CH01	0.8364*	0.02118*	12	5.7
CH02	0.8364*	0.06973*	12	5.7
CH03	0.8364*	0.1558*	12	5.9
CH04	0.8364*	0.04765*	12	5.7
CH05	0.8364*	0.07269*	12	5.8
CH06	0.8364*	0.05114*	12	6.5
CH07	0.8364*	0.1005*	12	5.5
CH08	0.8364*	0.07117*	12	6.8
CH09	0.8364*	0.1066*	12	5.5
CH10	0.8364*	0.03117*	12	6.0
CH11	0.8364*	0.03173*	12	5.5
CH12	0.8364*	0.04455*	12	5.8
CH13	0.8364*	0.01058*	12	5.5
CH14	0.8364*	0.2092*	12	6.7
CH15	0.8364*	0.1023*	12	6.7
CH16	0.8364*	0.002935*	12	5.5
CH17	0.8364*	0.06313*	12	6.7
CH18	0.8364*	0.04736*	12	5.5
CVG NEA00	1.098*	0.1511*	12	6.4
CVG NEA01	1.098*	0.01076*	12	5.5
CVG NEA02	1.098*	0.4239*	12	6.1
CVG NEA03	1.098*	0.1769*	12	5.5
CVG NEA04	1.098*	0.1757*	12	5.6
CVG NEA06	1.098*	0.2196*	12	5.6
Cyp00	0.9488*	1.378*	12	7.3
Cyp01	0.9488*	0.5321*	12	5.6
D-C01	0.8321*	0.006507*	12	5.5
D-C02	0.8321*	0.004338*	12	5.5
D-C04	0.8321*	0.004338*	12	5.5
D-C05	0.8321*	0.008771*	12	5.5
D-C06	0.8321*	0.01084*	12	5.5
D-C07	0.8321*	0.002169*	12	5.5
D-C08	0.8321*	0.004338*	12	5.5
D-C09	0.8321*	0.008676*	12	5.5
D-C10	0.8321*	0.004338*	12	5.5
D-C11	0.8321*	0.01301*	12	5.5
D-C12	0.8321*	0.002169*	12	5.5
D-C13	0.8321*	0.008771*	12	5.5
D-S00	0.9233*	0.03072*	12	5.6
D-S01	0.9233*	0.004088*	12	5.5
D-S02	0.9233*	0.1486*	12	6.2
D-S03	0.9233*	0.03764*	12	5.5
D-S04	0.9233*	0.07771*	12	6.4
D-S05	0.9233*	0.01586*	12	5.5
D-S06	0.9233*	0.01369*	12	5.8
D-S07	0.9233*	0.02456*	12	5.5
D-S08	0.9233*	0.004088*	12	5.5
D-S09	0.9233*	0.004088*	12	5.5
D-S10	0.9233*	0.05427*	12	5.8
D-S12	0.9233*	0.01228*	12	5.5
D-S13	0.9233*	0.0307*	12	5.5
D-S14	0.9233*	0.004088*	12	5.5
D-S15	0.9233*	0.004088*	12	5.5
D-S16	0.9233*	0.1427*	12	5.5
D-S17	0.9233*	0.03171*	12	5.5
D-S18	0.9233*	0.1399*	12	6.0
D-S19	0.9233*	0.004088*	12	5.5
D-S20	0.9233*	0.01229*	12	5.7
D-S21	0.9233*	0.004088*	12	5.5

Table 3. continued				
Title	<i>b</i>	<i>v</i>(3.8) [p.a.]	<i>h</i> [km]	<i>m</i>_{max}
D-S22	0.9233*	0.02456*	12	5.5
D-S24	0.9233*	0.03073*	12	5.7
F00	1.427*	0.1076*	12	5.5
F01	1.427*	0.2056*	12	5.5
F02	1.427*	0.08224*	12	5.5
F03	1.427*	0.002572*	12	5.5
F04	1.427*	0.04112*	12	5.5
F05	1.427*	0.002572*	12	5.5
F06	1.427*	0.08224*	12	5.5
F07	1.427*	0.4086*	12	5.7
F08	1.427*	0.1234*	12	5.5
F09	1.427*	0.2467*	12	5.5
F10	1.427*	0.04112*	12	5.5
F11	1.427*	0.04112*	12	5.5
F12	1.427*	0.02979*	12	5.5
F13	1.427*	0.08224*	12	5.5
F14	1.427*	0.01986*	12	5.5
F15	1.427*	0.08224*	12	5.5
F16	1.427*	0.1645*	12	5.5
F17	1.427*	0.2868*	12	5.6
F18	1.427*	1.165*	12	6.6
F19	1.427*	0.2043*	12	5.7
F20	1.427*	0.08224*	12	5.5
F21	1.427*	0.24*	12	6.3
Gr00	0.9191*	0.3221*	12	7.2
Gr01	0.9191*	1.307*	12	7.0
Gr02	0.9191*	0.5246*	12	7.6
Gr03	0.9191*	0.2605*	12	6.3
Gr04	0.9191*	1.367*	12	7.3
Gr05	0.9191*	2.038*	12	7.6
Gr06	0.9191*	1.228*	12	7.8
Gr07	0.9191*	1.157*	12	6.9
Gr08	0.9191*	0.5705*	12	6.7
Gr09	0.833	4.113	12	7.3
Gr10	0.9191*	3.048*	12	7.3
Gr11	0.9191*	1.293*	12	7.5
Gr12	0.9191*	0.7958*	12	7.3
Gr13	0.9191*	0.7045*	12	6.8
Gr14	0.8625	2.303	12	7.4
Gr15	0.9191*	0.9947*	12	7.3
Gr16	0.9191*	0.8452*	12	7.5
Gr17	0.9191*	0.7487*	12	5.7
Gr18	0.6724	1.92	12	7.7
Gr19	0.772	2.032	12	7.1
Gr20	0.9191*	0.8999*	12	6.9
Gr21	0.9191*	1.682*	12	7.3
Gr22	0.9191*	1.293*	12	7.3
Gr23	0.9191*	1.375*	12	7.3
Gr24	0.9191*	0.8547*	12	7.0
Gr25	0.7991*	0.5747*	80	7.1
Gr26	0.9191*	1.442*	12	7.3
Gr27	0.9191*	0.3112*	12	6.7
Gr28	0.9191*	0.347*	12	6.6
Gr29	1.089	3.732	12	7.3
Gr30	0.9191*	1.541*	12	7.5
Gr31	0.9191*	0.7545*	12	6.9
Gr32	0.7991*	0.3053*	130	6.3
Gr33	0.9191*	2.524*	12	8.3
Gr34	0.9191*	0.5471*	12	7.3
Gr35	0.9191*	1.505*	12	7.1
Gr36	0.9191*	0.9947*	12	7.3
Gr37	0.9191*	1.375*	12	7.8
Gr38	0.7991*	0.6523*	130	7.4

Table 3. continued				
Title	<i>b</i>	<i>v</i>(3.8) [p.a.]	<i>h</i> [km]	<i>m</i>_{max}
Gr39	0.7991*	0.2168*	80	7.7
Gr40	0.7991*	0.3822*	130	5.9
Gr41	1.069	12.79	12	8.3
Gr42	0.9191*	1.155*	12	7.5
Gr43	0.7991*	0.7505*	80	6.7
Gr44	0.9191*	1.515*	12	8.3
Gr45	0.9191*	0.7859*	12	8.1
Gr46	0.9191*	2.892*	12	6.6
Gr47	0.9457	3.289	12	8.1
Gr48	0.7991*	0.7796*	80	7.2
Gr49	0.9191*	1.616*	12	8.3
Gr50	0.9191*	1.515*	12	8.3
Gr51	1.228	15.93	12	6.8
Gr52	0.9191*	3.007*	12	6.6
Gr53	0.9191*	2.928*	12	8.3
Gr54	0.9191*	2.943*	12	7.3
Gr55	0.9191*	2.802*	12	6.4
Hu00	0.7048*	0.0943*	12	6.0
Hu01	0.7048*	0.01933*	12	5.6
Hu02	0.7048*	0.1247*	12	6.1
Hu03	0.7048*	0.004833*	12	5.6
Hu04	0.7048*	0.004829*	12	5.5
Hu05	0.7048*	0.02864*	12	5.8
Hu06	0.7048*	0.002893*	12	5.5
Hu07	0.7048*	0.03015*	12	5.6
Hu08	0.7048*	0.002893*	12	5.5
Hu09	0.7048*	0.009658*	12	5.5
Hu10	0.7048*	0.07456*	12	5.6
Hu11	0.7048*	0.05312*	12	5.5
Hu12	0.7048*	0.01017*	12	5.5
Hu13	0.7048*	0.009658*	12	5.5
Hu14	0.7048*	0.002893*	12	5.6
Hu15	0.7048*	0.002893*	12	5.6
Hu16	0.7048*	0.05696*	12	6.8
Hu17	0.7048*	0.02035*	12	5.5
Hu18	0.7048*	0.2163*	12	5.9
Ib00	0.8544*	0.04566*	12	5.5
Ib01	0.8544*	0.09683*	12	5.6
Ib02	0.8544*	0.04711*	12	5.8
Ib03	0.8544*	0.06288*	12	6.2
Ib04	0.8544*	0.06286*	12	6.0
Ib05	0.8544*	0.5696*	12	6.2
Ib06	0.8544*	0.129*	12	5.5
Ib07	0.8544*	0.2441*	12	6.2
Ib08	0.8544*	0.01786*	12	5.5
Ib09	0.8544*	0.2518*	12	7.2
Ib10	0.8544*	0.1689*	12	6.8
Ib11	0.8544*	0.1863*	12	7.4
Ib12	0.8544*	0.1075*	12	6.9
Ib13	0.8544*	0.5036*	12	7.2
Ib14	0.8544*	0.5924*	12	6.8
Ib15	0.8544*	0.1515*	12	7.2
Ib16	0.8544*	0.04606*	12	7.1
Ib17	0.8544*	0.1228*	12	7.0
Ib18	0.8544*	0.1826*	12	5.5
Ib19	0.8544*	1.321*	12	6.6
Ib20	0.8544*	0.8708*	12	8.8
Ib21	0.8544*	0.9099*	12	7.0
Is00	1.072*	6.995*	12	7.4
Is01	1.072*	0.4873*	12	6.0
Is02	1.072*	5.436*	12	6.1
Is03	1.072*	0.1158*	12	5.5
Is04	1.072*	1.239*	12	6.0

Table 3. continued				
Title	<i>b</i>	<i>v</i> (3.8) [p.a.]	<i>h</i> [km]	<i>m</i> _{max}
Is05	1.072*	0.9746*	12	6.0
Is06	1.072*	0.2895*	12	5.5
Is07	1.072*	2.484*	12	5.7
Is08	1.072*	7.483*	12	7.4
Is09	1.072*	2.263*	12	6.2
Mag00	1.114*	0.1022*	12	5.5
Mag01	1.114*	0.4904*	12	7.3
Mag02	1.114*	0.795*	12	6.1
Mag03	1.114*	2.513*	12	6.4
Mag04	1.114*	0.1537*	12	5.5
Mag05	1.114*	0.3074*	12	5.5
Mag06	1.114*	5.752*	12	7.6
Mag07	1.114*	0.1537*	12	5.5
Mag08	1.114*	0.9559*	12	7.6
Mag09	1.114*	5.675*	12	6.8
Mag10	1.114*	1.113*	12	7.2
Mag11	1.114*	0.6947*	12	5.7
Mag12	1.114*	0.1022*	12	5.5
Mag13	1.114*	0.265*	12	6.1
Mag14	1.114*	0.1345*	12	7.0
Mag15	1.114*	0.2044*	12	5.5
Mag16	1.114*	0.3074*	12	5.5
Mag17	1.114*	0.2242*	12	7.0
Mag18	1.114*	0.1537*	12	5.5
Mag19	1.114*	0.433*	12	6.7
Mag20	1.114*	1.724*	12	7.0
Mag21	1.114*	0.03008*	12	6.1
Mag22	1.114*	1.757*	12	5.9
Mag23	1.114*	0.1537*	12	5.5
Mag24	1.114*	0.3074*	12	5.5
Mag25	1.114*	0.9275*	12	6.1
Mag26	1.114*	0.2044*	12	5.5
Mag27	1.114*	0.1022*	12	5.5
Mag29	1.114*	0.7685*	12	5.5
Mag30	1.097	4.585	12	7.3
Mag32	1.114*	0.01786*	12	5.5
Mag33	1.114*	0.4309*	12	7.0
Mag34	1.114*	0.1537*	12	5.5
Mag35	1.114*	0.2946*	12	6.1
Mag36	1.114*	0.3927*	12	5.5
Mag37	1.114*	0.03023*	12	5.7
Mag38	1.114*	0.0449*	12	6.7
NA00	1.349	49.78	12	7.3
NWB00	0.8397*	0.1015*	12	6.8
NWB01	0.8189	0.5802	12	6.8
NWB02	0.8397*	0.05073*	12	6.8
NWB03	0.8397*	0.1348*	12	5.6
NWB04	0.8397*	0.372*	12	6.8
NWB05	0.8397*	0.2018*	12	6.8
NWB06	0.8397*	0.2417*	12	6.0
NWB07	0.8397*	0.4766*	12	6.8
NWB08	0.8397*	0.07759*	12	5.5
NWB09	0.8397*	0.4397*	12	6.8
NWB10	0.9299	0.4478	12	6.8
NWB11	0.8397*	0.1196*	12	6.8
NWB12	0.8878	0.4526	12	6.8
NWB13	0.8397*	0.09729*	12	5.5
NWB14	0.8397*	0.2317*	12	6.8
NWB15	0.8397*	0.2861*	12	6.1
NWB16	0.8397*	0.2706*	12	6.8
NWB17	0.8397*	0.2198*	12	6.8
NWB18	0.8397*	0.1638*	12	5.7
NWB19	0.8397*	0.743*	12	7.0

Table 3. continued				
Title	<i>b</i>	<i>v</i>(3.8) [p.a.]	<i>h</i> [km]	<i>m</i>_{max}
PP00	1.678*	0.2551*	12	5.5
PP01	1.678*	8.423*	12	7.1
PP02	1.678*	6.404*	12	6.6
PP03	1.678*	0.06505*	12	5.5
PP04	1.678*	1.531*	12	7.2
PP05	1.678*	4.085*	12	6.9
PP06	1.678*	2.598*	12	6.0
PP07	1.678*	2.818*	12	6.4
PP08	1.678*	1.153*	12	5.5
PP09	1.678*	1.532*	12	6.8
PP10	1.678*	0.102*	12	5.5
PP11	1.678*	3.408*	12	5.8
PP12	1.678*	1.818*	12	6.0
PP13	1.678*	1.039*	12	6.0
PP14	1.678*	0.2882*	12	5.5
PP15	1.678*	2.305*	12	5.5
PP16	1.678*	0.8645*	12	5.5
Pyr00	1.313*	0.4219*	12	6.4
Pyr01	1.313*	0.1887*	12	5.5
Pyr02	1.313*	0.2411*	12	6.4
Pyr03	1.313*	0.08607*	12	6.8
Ro-C00	0.6982*	0.1121*	12	6.5
Ro-C01	0.6982*	0.1679*	12	7.1
Ro-C02	0.6982*	0.05104*	12	6.2
Ro-C03	0.6982*	0.03755*	12	5.5
Ro-C04	0.6982*	0.01458*	12	6.2
Ro-C05	0.6982*	0.06298*	12	7.0
Ro-C06	0.6982*	0.1189*	12	6.8
Ro-C07	0.6982*	0.0843*	12	5.5
Ro-C08	0.6982*	0.1216*	12	5.9
Ro-C09	0.6982*	0.09744*	12	7.5
Ro-C10	0.6982*	0.04957*	12	6.4
Ro-D00	0.6573	4.279	143	7.9
SAC00	1.011*	0.1411*	12	5.5
SAC01	1.011*	0.9601*	12	6.5
SAC02	1.011*	0.1521*	12	7.0
SAC03	1.011*	0.5413*	12	7.5
SAC04	1.011*	0.3966*	12	6.9
SAC05	1.011*	0.3713*	12	6.2
SAC06	1.011*	0.2527*	12	5.5
SAC07	1.011*	1.084*	12	7.3
SAC08	1.011*	0.06747*	12	5.9
SAC09	1.011*	0.4043*	12	6.5
SAC10	1.011*	0.7388*	12	7.3
SAC11	1.011*	0.2788*	12	5.8
SAC12	1.011*	0.239*	12	6.9
SAC13	1.011*	0.06572*	12	6.4
SAC14	1.449	8.036	12	7.4
SAC15	1.011*	0.3691*	12	7.2
SAC16	1.011*	0.2615*	12	7.2
SAC17	1.011*	0.1591*	12	6.2
Sic00	1.346*	2.335*	12	6.4
Sic01	1.346*	0.7597*	12	5.9
Sic02	1.346*	1.497*	12	6.6
Sic03	1.346*	1.121*	12	6.2
Sic04	1.346*	0.3343*	12	6.3
Sic05	1.346*	0.3948*	12	6.6
Sic06	1.346*	0.8081*	12	7.7
Sic07	1.346*	0.4876*	12	6.9
Sic08	1.346*	1.586*	12	5.9
Sk/Pl/Cz00	0.8321*	0.02621*	12	5.5
Sk/Pl/Cz01	0.8321*	0.00714*	12	5.5
Sk/Pl/Cz02	0.8321*	0.02856*	12	5.5

Table 3. continued				
Title	<i>b</i>	$\nu(3.8)$ [p.a.]	<i>h</i> [km]	m_{max}
Sk/Pl/Cz03	0.8321*	0.04941*	12	6.1
Sk/Pl/Cz05	0.8321*	0.1737*	12	6.2
Sk/Pl/Cz06	0.8321*	0.1249*	12	6.0
Sk/Pl/Cz07	0.8321*	0.04284*	12	5.5
Sk/Pl/Cz08	0.8321*	0.03932*	12	5.5
Tr-E00	0.6603	1.428	12	7.8
Tr-E01	0.9585	11.15	12	7.7
Tr-E02	0.9912	2.682	12	7.0
Tr-E03	0.8542	2.571	12	7.5
Tr-E04	0.9478	3.414	12	7.7
Tr-W00	1.012*	3.672*	12	7.2
Tr-W01	1.012*	2.909*	12	7.8
Tr-W02	1.012*	2.269*	12	7.8
Tr-W03	1.012*	2.606*	12	7.8
Tr-W04	1.012*	1.524*	12	6.1
Tr-W05	1.264	8.651	12	7.4
Tr-W06	1.012*	1.642*	12	7.3
Tr-W07	1.012*	0.8981*	12	6.8
Tr-W08	1.012*	2.068*	12	7.3
Tr-W09	1.012*	2.371*	12	7.4
Tr-W10	1.012*	6.131*	12	7.2
WM00	1.231*	0.1571*	12	5.5
WM01	1.231*	2.409*	12	5.6

5. The sanity check of the derived parameters in terms of a preliminary seismic hazard map

The derived earthquake model has been applied for a probabilistic seismic hazard assessment (PSHA) for the entire study area. The aim of this hazard calculation is basically to perform a first rough sanity check and not to provide any final hazard map. This part of the study is divided (1) in the selection of suitable ground motion prediction equations (GMPEs) and (2) in suggested minor modifications in the source zone model in the Maghreb to get more reliable PSHA results due to modifications in the nowadays used seismicity data.

It is not intended here to perform an extensive PSHA using logic trees and further refinements. This preliminary approach also does not make use of finite fault effects for events with $M_w \geq 7$. Since we want to compare our PSHA results with previous ones, which are also not based on finite fault calculations, it was not part of the study.

(1) Selection of suitable GMPEs

The seismicity in the study area consists of mostly shallow crustal earthquakes and in two subregions only a notably seismic activity occurs at intermediate depth. These are the (a) Vrancea region in Romania which represents the last remnants of a subducted slab and (b) the Hellenic arc or the Aegean subduction zone.

For the areas with shallow crustal seismicity, which represent the vast majority of SSZs,

we apply the GMPE by *Akkar & Bommer* (2010). It constitutes the most recent GMPE based on European, Mediterranean and Near East strong motion data.

For the two sub-areas with intermediate depth seismicity we apply different GMPEs.

(a) The Vrancea region with devastating $M \geq 7$ earthquakes in the past shows a very peculiar anisotropic attenuation pattern of ground motion. It therefore requires the use of a specific GMPE. Up to now the existing high quality ground motion data are too scarce to establish a specific reliable relation. Therefore, the published GMPEs for this region combine the few PGA or PGV data and/or wave field simulations with the pronounced anisotropic attenuation of macroseismic intensity data observed from the large events of the last century (*Sokolov et al.* 2008 and references therein). Here, the most recent M_w calibrated intensity prediction equation from *Sørensen et al.* (2010) together with an area-specific linear regression relation between intensity and $\log(\text{PGA})$ (*Sørensen et al.* 2007) has been used.

(b) The *Atkinson & Boore* (2003) GMPE for subduction zones was chosen for the Hellenic arc intermediate depth zones. It is relatively recent and generally applicable to this type of zones worldwide. This GMPE has also recently been applied by *Weatherill & Burton* (2010) for the Hellenic arc. Only in-slab type events were considered in the calculations since the subduction zone is only characterized in the SESAME model for intermediate depth events. At these depths intraplate events occur (e.g. see *Lay & Wallace* 1995).

Since the *Akkar & Bommer* (2010) model uses the Joyner-Boore distance a distance metric conversion procedure according to *Scherbaum* (2004) has been applied but in a form which is more suitable for complex numerical procedures (*Grünthal et al.* 2009d). This enables the introduction of the focal depths in the SSZs, which is crucial in the large low seismicity areas within Europe. For reasons of comparison with previous maps a lower magnitude threshold in the integration of $M_w = 4.5$ has been introduced. The aleatory uncertainty in the GMPEs has been limited to $\pm 2\sigma$. All GMPEs were applied for rock site conditions.

(2) Modification of SSZs in the Maghreb for better adjusting the modified seismicity data

The reason for introducing the minor modifications in the Maghreb are basically two SSZs in the Atlas region of Morocco and Algeria (Mag31, Mag34), which were delineated originally in SESAME to encompass areas of higher seismic activity than the surroundings show. According to the current seismicity data file these SSZs are either “empty” (Mag31) from any seismicity now according to the applied magnitude threshold and completeness pattern or show much lower activity rate than the surroundings (Mag34). This would result in some kind of “holes” in the hazard map. In order to avoid this, both SSZs have simply been deleted from the hazard analysis. Their areas were added to the surroundings of the source Mag30.

The resulting hazard map (Figure 17) is calculated with the modified FRISK88M software (*Risk Engineering Ltd.* 1997) in terms of PGA to enable comparisons with previous maps like the ones produced in the frame of GSHAP (*Grünthal et al.* 1999a, b) and with the

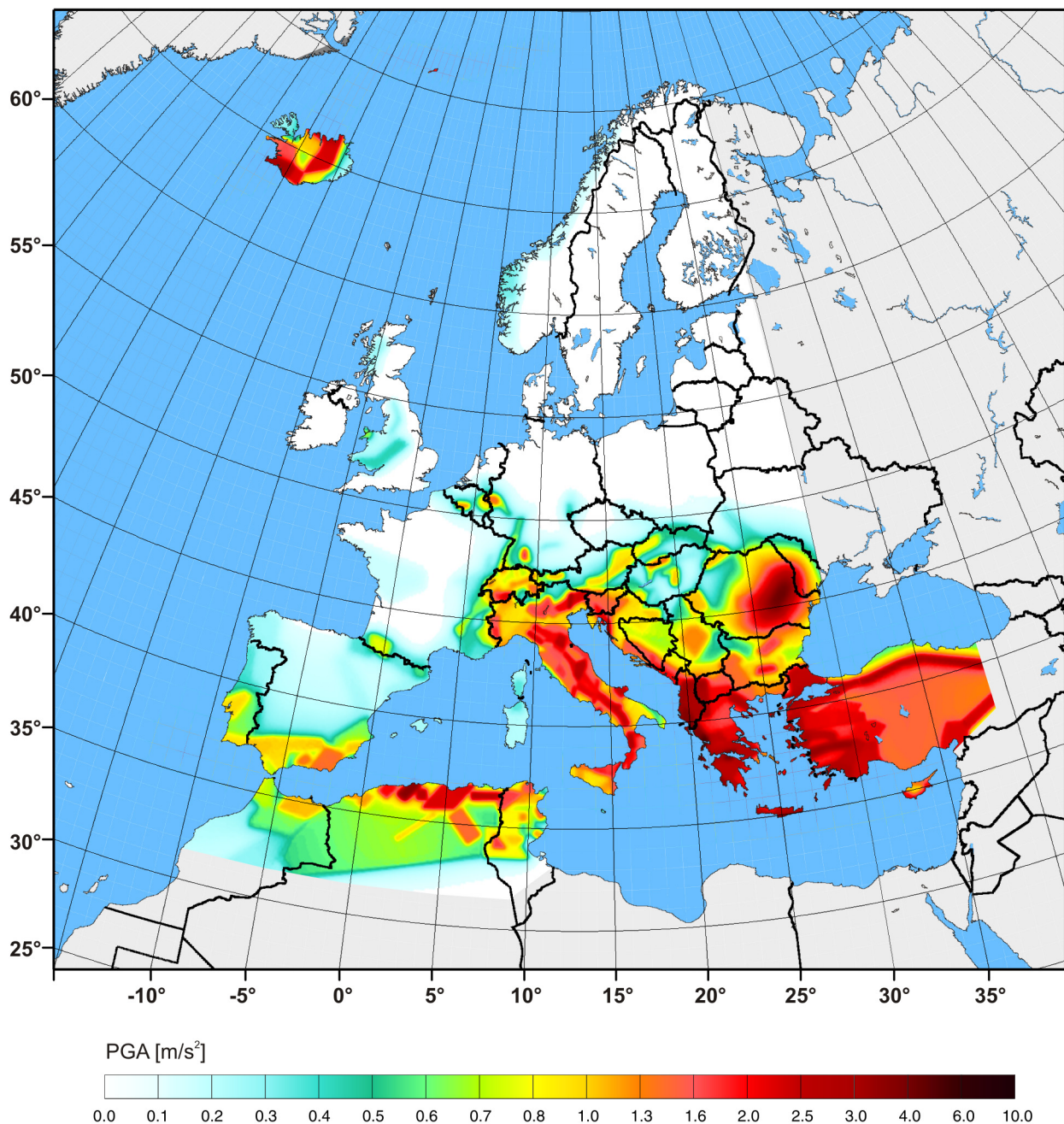


Figure 17. Hazard map computed according to the seismic source zone data of table 3 using recent GMPEs for the study area (Akkar & Bommer 2010; Atkinson & Boore 2003; Sørensen et al. 2010).

SESAME map itself (Jiménez et al. 2003). The map very well reflects the spatial variation in seismicity within the study area. It can be concluded that the underlying earthquake model should be suitable for generalized applications.

Any comparison with the two previous European approaches in seismic hazard assessment (GSHAP, SESAME*) has to consider that the used GMPEs for calculating the three European maps are completely different. Here, the calculations have been performed for rock conditions, while the GSHAP and the SESAME results are given for stiff soil. Notwithstanding the facts the new preliminary map is rather similar to the previous ones. In general,

* Note, the SESAME map could be compared qualitatively only.

with some exceptions, the resulting PGA values are now slightly lower. Exceptions can be seen in Vrancea, Central Anatolia and in the Maghreb area with higher PGA values in the new map. The PGA calculated for the Iberian peninsula (except those for southern Spain) steadily decrease from GSHAP to SESAME and finally in the new map.

6. Conclusions

In conclusion, this study presents a European earthquake model which, in a homogeneous way, treats all of Europe and the Maghreb with respect to catalogue completeness, activity rates and m_{max} . The comprehensive model is basically built on the progress made in homogeneous and harmonized earthquake cataloguing with the data files CENEC (Grünthal et al. 2009a) and EMEC (Grünthal & Wahlström 2009). This is the first earthquake model released for Europe and the western Mediterranean. In comparison to the old but never published SESAME model several background source zones have been introduced in the Mediterranean area. Iceland and adjacent parts of the North Atlantic ridge have newly constructed SSZs. The determination of depths for the SSZs was not a straightforward task and, therefore, standard depths are used for the shallow sources and average values of earthquake depths for the intermediate depth sources. According to a first sanity check in form of an elementary seismic hazard calculation the derived earthquake model proved to be suitable for generalized applications. In general, the here presented hazard is slightly lower but reflects results from previous studies. Some areas with increased PGA, compared to the SESAME model, can be observed in Vrancea, Central Anatolia and the Maghreb area.

References

- Akkar S, Bommer JJ (2010) Empirical Equations for the Prediction of PGA, PGV, and Spectral Accelerations in Europe, the Mediterranean Region, and the Middle East. *Seismological Research Letters* 81 (2): 195-206.
- Atkinson G M, Boore D M (2003) Empirical Ground-Motion Relations for Subduction-Zone Earthquakes and Their Application to Cascadia and Other Regions. *Bulletin of the Seismological Society of America* 93 (4): 1703-1729.
- Burkhard M, Grünthal G (2009) Seismic source zone characterization for the seismic hazard assessment project PEGASOS by the Expert Group 2 (EG 1b). *Swiss Journal of Geosciences* 102 (1): 149-188.
- Coppersmith, KJ (1994) Conclusions regarding maximum earthquake assessment. In: *The Earthquakes of Stable Continental Regions, Vol. 1: Assessment of large Earthquake Potential*. Electric Power Research Institute (EPRI) TR-102261-V1, 6-1 – 6-24.
- Cornell CA (1994) Statistical analysis of maximum magnitudes. In: *The Earthquakes of Sta-*

- ble Continental Regions, Vol. 1: Assessment of large Earthquake Potential. Electric Power Research Institute (EPRI) TR-102261-V1, 5-1 - 5-27.
- CPTI Working Group (2004) *Catalogo Parametrico dei Terrimoti Italiani*, versione 2004 (CPTI04). Istituto Nazionale di Geofisica e Vulcanologica, Milan, Italy (<http://emidius.mi.ingv.it/CPTI04/>)
- Giardini D, Grünthal G, Shedlock KM, Zhang P (1999) The GSHAP Global Seismic Hazard Map. *Annali di Geofisica* 42(6): 1225-1230.
- Grünthal G, GSHAP Region 3 Working Group (1999a) Seismic hazard assessment for central, north and northwest Europe: GSHAP Region 3. *Annali di Geofisica* 42 (6): 999-1011.
- Grünthal G, Wahlström R (2006) New generation of probabilistic seismic hazard assessment for the area Cologne/Aachen considering the uncertainties of the input data. *Natural Hazards* 38(1-2): 159-176.
- Grünthal G, Wahlström R (2009) A harmonized seismicity data base for the Euro-Mediterranean region. In: *Cahiers du Centre Européen de Géodynamique et de Séismologie* 28, Proceedings of the 27th ECGS Workshop "Seismicity Patterns in the Euro-Med Region", Luxembourg, 15-21.
- Grünthal G, Bosse C, Stromeyer D (2009d) Die neue Generation der probabilistischen seismischen Gefährdungseinschätzung der Bundesrepublik Deutschland: Version 2007 mit Anwendung für die Erdbeben-Lastfälle der DIN 19700:2004-07 'Stauanlagen'. Scientific Technical Report STR 09/07, Deutsches GeoForschungsZentrum, Potsdam, 81 pp.
- Grünthal G, Wahlström R, Stromeyer D (2009a) The unified catalogue of earthquakes in central, northern, and northwestern Europe (CENEC) - updated and expanded to the last millennium. *Journal of Seismology* 13 (4): 517-541.
- Grünthal G, Wahlström R, Stromeyer D (2009c) Harmonization check of M_w within the central, northern, and northwestern European earthquake catalogue (CENEC). *Journal of Seismology* 13(4): 613-632.
- Grünthal G, Bosse C, Sellami S, Mayer-Rosa D, Giardini D (1999b) Compilation of the GSHAP regional seismic hazard for Europe, Africa and the Middle East. *Annali di Geofisica* 42 (6): 1215-1223.
- Grünthal G, Hakimhashemi A, Schelle H, Bosse C, Wahlström R (2009b) The long-term temporal behaviour of the seismicity of the Dead Sea Fault Zone and its implication for time-dependent seismic hazard assessments. Scientific Technical Report STR 09/09, GFZ German Research Centre for Geosciences, Potsdam, 45 pp.
- Gulia L, Meletti C (2008) Testing the b-value variability in Italy and its influence on Italian PSHA. *Bollettino di geofisica teorica ed applicata* 49 (1): 59-76.
- Gutenberg B, Richter CF (1954) *Seismicity of the Earth*, Princeton University Press, Princeton, N. J., 310 pp.
- Jiménez M-J, Giardini D, Grünthal G (2003) The ESC-SESAME unified hazard model for the European-Mediterranean region. *EMSC/CSEM Newsletter* 19: 2-4.
- Jiménez M-J, Giardini D, Grünthal G, SESAME Working Group (2001) Unified seismic hazard modelling throughout the Mediterranean region. *Bollettino di geofisica teorica ed appli-*

- cata 42 (1-2): 3-18.
- Kijko A, Graham G (1998) Parametric historic procedure for probabilistic seismic hazard analysis. Part 1: Estimation of maximum regional magnitude m_{max} . *Pure and Applied Geophysics* 152 (3): 413-442.
- Lay C, Wallace TC (1995) *Modern Global Seismology*. Academic Press, 521 pp.
- Meletti C, Galadini F, Valensise G, Stucchi M, Basili R, Barba S, Vannucci G, Boschi E (2008) A seismic source zone model for the seismic hazard assessment of the Italian territory. *Tectonophysics* 450 (1-4): 85-108.
- Musson, RMW (1999) Probabilistic seismic hazard map for the North Balkan region. *Annali di Geofisica*, 42 (6): 1109-1124.
- Musson RMW, Sargeant, SL (2007) Eurocode 8 seismic hazard zoning maps for the UK. Technical Report CR/07/125, British Geological Survey, Edinburgh, 62 pp.
- NORSAR, NGI (1998) Seismic zonation for Norway. Technical Report, NFR/NORSAR, Kjeller, Norway. 162 pp.
- Papiouannou C, Papazachos BC (2000) Time-independent and time-dependent seismic hazard in Greece based on seismogenic sources. *Bulletin of the Seismological Society of America* 90 (1): 22-33.
- Rebez A, Slejko D (2004) Introducing epistemic uncertainties into seismic hazard assessment for the broader Vittorio Veneto area (n. E. Italy). *Bolletino di Geofisica Teorica ed Applicata* 45 (4): 305-320.
- Risk Engineering Ltd. (1997) FRISK88Mc Users Manual, updated version 1.70.
- Scherbaum F, Schmedes J, Cotton F (2004) On the conversion of source-to-site distance measures for extended earthquake source models. *Bulletin of the Seismological Society of America* 94(3): 1053-1069.
- Slejko D, Peruzza L, Rebez A (1998) Seismic hazard maps of Italy. *Annali di Geofisica* 41 (2): 183-214.
- Sokolov V, Bonjer K-P, Wenzel F, Grecu B, Radulian M (2008) Ground-motion prediction equations for the intermediate depth Vrancea (Romania) earthquakes. *Bulletin of Earthquake Engineering* 6: 367-388.
- Sørensen M, Stromeyer D, Grünthal G (2007) Generation of area-specific relationships between ground motion parameters (PGA, PGV) at certain sites, magnitude M and distance R to the causative fault and site intensities in terms of EMS-98. SAFER report, Deliverable No. 4.1 (due date: 15.06.2007), 19 pp.
- Sørensen M, Stromeyer D, Grünthal G (2010) A macroseismic intensity prediction equation for intermediate depth earthquake in the Vrancea region, Romania. *Soil Dynamics and Earthquake Engineering* 30 (11): 1268-1278.
- Suckale J, Grünthal G (2009) A probabilistic seismic hazard model for Vanuatu. *Bulletin of the Seismological Society of America* 99 (4): 2108-2126.
- Wahlström R, Grünthal G (2001) Probabilistic seismic hazard assessment (horizontal PGA) for Fennoscandia using the logic tree approach for regionalization and nonregionalization models. *Seismological Research Letters* 72 (1): 33-45.

Weatherill G, Burton PW (2010) An alternative approach to probabilistic seismic hazard analysis in the Aegean region using Monte Carlo simulation. *Tectonophysics* 492 (1-4): 253-278.

Weichert DH (1980) Estimation of the earthquake recurrence parameters for unequal observations periods for different magnitudes. *Bulletin of the Seismological Society of America* 70 (4): 1337-1346.

